Rheology of cement grout – Ultrasound based in-line measurement technique and grouting design parameters

Mashuqur Rahman

Doctoral Thesis
Department of Civil and Architectural Engineering
Division of Soil and Rock Mechanics
KTH Royal Institute of Technology
SE- 100 44, Stockholm
Sweden
November, 2015

TRITA-JOB PHD 1021
ISSN 1650-9501
ISRN KTH

Doctoral dissertation to be defended in F3, Lindstedtsvägen 26, KTH Royal Institute of Technology, Stockholm, Sweden, on 18th of November 2015, at 13.00

Faculty opponent: Prof. Olafur H. Wallevik, Reykjavik University, Iceland.
Evaluation Committee members:
Prof. Mikael Rinne, Aalto University, Finland.
Prof. Eivind Grøv, University of Science and Technology in Trondheim (NTNU), Norway.
Dr. Annika Gram, Swedish Cement and Concrete Research Institute.

Summary

Grouting is performed in order to decrease the permeability and increase the stiffness of the material, especially soil and rock. For tunnelling and underground constructions, permeation grouting is done where cement based materials are pumped inside drilled boreholes under a constant pressure, higher than the ground water pressure. The aim of permeation grouting is to reduce the water flow into tunnels and caverns and to limit the lowering of the surrounding groundwater table. Cement based materials are commonly used as grout due to their availability and lower costs. To obtain a proper water sealing and reduce the lowering of the ground water table, a desired spread of grout must be achieved and the rheology of the cement grout is the governing factor for estimating the required spread. Rheological properties of cement grout such as viscosity and yield stress are commonly measured off-line using laboratory instruments, and some simple tools are available to make field measurements. Although the rheological properties of the grout that is used play a fundamental role in design and execution, no method has yet been developed to measure these properties in-line in field work. In addition to the real time measurement, there is no standard method for determining the yield stress for grouting applications. Despite the common usage of Bingham model fitting to determine the yield stress, the range of shear rate is often not specified or is neglected.

In this work, an in-line rheometry method combining the Ultrasound Velocity Profiling (UVP) technique with Pressure Difference (PD) measurements, known as "UVP+PD", was successfully tested for continuous in-line measurements of concentrated micro cement based grouts. A major obstacle of using the ultrasound based methodology was the transducers, which would be capable of emitting sufficient acoustic energy and can be used in field conditions. The transducer technology was developed in a parallel project and the Flow-Viz industrial rheometer was found to be capable of detail measurement of the velocity profiles of cement grout. The shape of the velocity profiles was visualized, and the change in the shape of the profiles with concentration and time was observed. The viscosity and yield stress of the grout were determined using rheological models, e.g. Bingham and Herschel-Bulkley. In addition, rheological properties were determined using the non-model approach (gradient method) and the tube viscometry concept and were compared with results obtained using the rheological models. The UVP+PD method was found to be capable of determining the rheological behavior of cement grout regardless of the rheological model.

The yield stress of cement grout was investigated using off-line rheometry techniques and UVP+PD in-line measurements. Tests were performed applying different shear histories and it was found that two ranges of yield stress indeed exist. Therefore, the design value of yield stress should be chosen with respect to the prevailing shear rate at the grout front for the required spread of grout. In addition, an appropriate shear rate range should be used when a Bingham fitting is done to determine the yield stress. In order to estimate the shear rate, plug thickness and velocity for one dimensional and two dimensional geometry, a non-dimensional nomogram was developed. The advantage of using the nomogram is that it does not depend on the applied pressure and the rheological properties of the grout and can therefore, be used as a simple design tool. Analytical approaches were used for the estimation and good agreements were found with numerical calculations and experimental results.

In conclusion, in this work, it was found that it is possible to continuously measure the velocity profiles and determine the change of the rheological properties of cement grout using the ultrasound based UVP+PD method under field conditions. The yield stress was also investigated and it was found that two range of yield stress exist depending on the prevailing shear rate of the grout, which should be used for designing the grouting time at different conditions. In order to decide the design value of yield stress for grouting applications, a non-dimensional nomogram was developed that can be used to estimate the plug thickness, shear rate and velocity of the grout.

Keywords: grouting, grouting design, cement grout, Bingham number, shear rate, plug flow, thixotropy, yield stress, in-line rheology, UVP+PD, Flow-Viz, viscosity bifurcation, aging, off-line rheometry, pump characteristics

Sammanfattning

Injektering i jord och berg utförs vanligen för att minska dess permeabilitet och för att göra materialet styvare. I tunnlar och underjordsanläggningar utförs arbetet genom att pumpa cementbaserade injekteringsmedel från borrade hål in i formationen, med ett tryck som överskrider rådande vattentryck. Syftet med injekteringen är att minska inflödet av vatten in i anläggningen och att minimera risken för en avsänkning av den omkringliggande naturliga grundvattennivån. Cementbaserade medel används ofta på grund av dess tillgänglighet och relativt låga kostnad. För att erhålla en effektiv tätning krävs en bra spridning av injekteringsbruket vilket påverkas av dess reologiska egenskaper. De reologiska egenskaperna, såsom viskositet och flytgräns, mäts vanligtvis i laboratorium och i viss mån med enkla metoder i fält. Trots att egenskaperna är av fundamentala då det gäller design och utförande, finns det idag ingen metod att mäta egenskaperna kontinuerligt i fält under utförandet. Det finns idag inte heller någon standardmetod för att fastställa injekteringsbrukets flytgräns eller dess variation med tiden. Trots att Bingham modellen används flitigt idag för att med kurvanpassning uppskatta flytgränsen finns det inga direktiv över vilket spann som den linjära anpassningen skall göras.

I föreliggande projekt har en in-line metod (UVP+PD) som kombinerar mätning av hastighetsprofilen med ultraljud (Ultra Sound Velocity Profiling – UVP) och mätning av tryckfallet (Pressure Difference – PD), använts. En utmaning inom projketet har varit att finna ultraljudsgivare som kan alstra tillräckligt med akustisk energi och som dessutom går att använda under fältlika förhållanden. Utveckling av givare har skett parallellt med det övriga arbetet inom projektet och den senaste industriella reometern, Flow-Viz, har visat sig kapabel att mäta hastighetsprofiler på vanligen använda cementbaserade injekteringsmedel. Hastighetsprofilerna har visualiserats och deras förändring som funktion av cementkoncentration har demonstrerats. Viskositet och flytgräns har utvärderats genom anpassning till olika reologiska modeller, såsom Bingham och Herschel-Bulkley. I tillägg har egenskaperna utvärderats genom en direkt bestämning utifrån hastighetsprofilerna vilket sedan jämförts med de reologiska modellerna. UVP+PD metodiken har visats sig kunna bestämma de reologiska parametrarna oavsett användandet av någon reologisk modell.

Flytgränsen hos cementbaserade injekteringsmedel har förutom UVP+PD även utvärderats med hjälp av konventionella reometrar. Försök har gjorts med olika grader av omrörning och det har visat sig att det existerar två olika nivåer av flytgräns beroende på historiken före mätning. Detta innebär att det valda värdet i en designsituation skall väljas beroende på rådande deformationshastighet i formationen som injekteras. Dessutom måste ett relevant spann av deformationshastighet, över vilken den linjära approximation för Bingham modellen görs, specificeras för att erhålla ett representativt värde på flytgränsen.
För att underlätta projekteringsarbetet vid injektering har ett dimensionslöst nomogram framtagits för uppskattning av deformationshastighet, pluggtjocklek och hastighet för endimensionellt och tvådimensionellt flöde. Fördelen med nomogrammet är att det är oberoende av tryck och medlets reologiska egenskaper och kan därför användas generellt som ett projekteringsverktyg. Nomogrammet har validerats mot numeriska beräkningar och laboratorieförsök med gott resultat.

En slutsats från detta projekt är att det går att mäta de reologiska egenskaperna på cementbaserade injekteringsmedel med ultraljud, kontinuerligt, under pågående injektering i fält. En annan slutsats är att det existerar två olika nivåer på flygräns, beroende på vilken grad av omrörning som bruket har utsatts för. Ett dimensionslöst nomogram har tagits fram inom projektet för att underlätta valet av rätt nivå vid olika omständigheter. Ur nomogrammet kan deformationshastighet, pluggtjocklek och hastighet bestämmas vid en viss tidpunkt.

Nyckelord: injektering, injekteringsdesign, cementbruk, Bingham number, deformationshastighet, pluggflöde, tixotropi, flytgräns, in-line reometri, UVP+PD, Flow-Viz, viskositets bifurkation, åldring, off-line reometri, pumpkaraktäristika.

Preface

The work presented in this thesis was performed at the Division of Soil and Rock Mechanics, KTH Royal Institute of Technology, and was supervised by Adj. Professor Ulf Håkansson. Funding for the project was provided by the Swedish Rock Engineering Research Foundation (BeFo), The Swedish Research Council (FORMAS) and The Development Fund of the Swedish Construction Industry (SBUF), who are gratefully acknowledged. The support of AtlasCopco in providing the LOGAC™ flow meter and Cementa AB in providing the cement grout is highly appreciated.

I am sincerely grateful to my supervisor, Ulf Håkansson, for providing valuable support and guidance. Laboratory work would not have been possible without the support of my co supervisor, Johan Wiklund, at the SP Technical Research Institute of Sweden. Special thanks to Professor Stefan Larsson for valuable advice and discussions. Members of the reference group - Thomas Dalmalm (Trafikverket), Rolf Christiansson (SKB), Staffan Hintze (NCC), Kyösti Tutti (Skanska), Tommy Ellisson (Besab), Per Tenborg (BeFo), Lars Hässler (Golder Associates), Professor Håkan Stille and Mats Holmberg are gratefully acknowledged for their suggestions and helpful scientific discussions. Further acknowledgements are directed to my colleagues at the Division of Soil and Rock Mechanics.

Finally, my gratitude goes to my parents in Bangladesh, my wife Ananna and son Ayman for their support, encouragement and allowing me to work continuously during countless weekends, vacation periods.

Stockholm, November 2015
Mashuqur Rahman

List of Publications

This doctoral thesis is based on the following five interrelated papers, attached as appendices of the thesis.

Paper I

Wiklund, J., Rahman, M., Håkansson, U., 2012. In-line rheometry of micro cement based grouts - A promising new industrial application of the ultrasound based UVP+PD method. *Applied Rheology 22, 42783.*

Paper II

Rahman, M., Håkansson, U., Wiklund, J., 2015. In-line rheological measurements of cement grouts: Effects of water/cement ratio and hydration. *Tunnelling and Underground Space Technology 45 (34-42).*

Paper III

Rahman, M., Wiklund, J., Kotze', R; Håkansson, U., 2015. Yield stress of cement grout. *Submitted to the journal Tunnelling and Underground Space Technology.*

Paper IV

Rahman, M., Hässler, L., Håkansson, U., 2015. Cement grouting design – a nomogram for velocity, plug thickness and shear rate. *Submitted to the journal Rock Mechanics and Rock Engineering.*

Paper V

Rahman, M., Håkansson, U., Wiklund, J., 2012. Grout pump characteristics evaluated with the Ultrasound Velocity profiling. *In: Proceeding of ISRM International Symposium, EUROCK, 28th-30th May, Stockholm.*

Additional papers relevant for the work

I. Håkansson, U., Rahman, M., 2009. Rheological properties of cement based grouts using the UVP-PD method. *In: Proceeding of Nordic Symposium of Rock Grouting, Helsinki.*

II. Håkansson, U., Rahman, M., Wiklund, J., 2012. In-line measurements of rheological properties of cement based grouts- Introducing the UVP-PD method. *In: Proceeding of 4th International Conference on Grouting and Deep Mixing, New Orleans. ASCE, Geotechnical Special Publication No. 228, Vol. 1, 1023-1034.*

III. Rahman, M., Håkansson, U., Wiklund, J., 2012. Application of the Ultrasound Velocity Profiling+ Pressure Difference (UVP+ PD) method in cement based grouts. *In: Proceedings of 8th International Symposium on Ultrasonic Doppler Methods for Fluid Mechanics and Fluid Engineering, Dresden.*

IV. Rahman, M., Håkansson, U., 2013. In-line Ultrasound Based Rheology – A New Tool for the Measurement of Flow and Rheological Properties of Cement Based Grout. *In: Proceedings of 47th US Rock Mechanics/Geomechanics Symposium, San Francisco, California, 23rd – 26th June, American Rock Mechanics Association (ARMA), 1738-1746.*

V. Rahman M., 2013. In-line rheology of cement grouts – Feasibility study of an ultrasound based non-invasive method. *BeFo Report No. 123.*

List of Symbols

b	Fracture aperture
B_N	Bingham number
$\frac{dI_D}{dt_D}$	Non-dimensional velocity
He	Hedström number
I	Spread of grout
I_D	Relative spread of grout
$I_{D,Pipe}$	Relative spread of grout for a pipe
$I_{D,channel}$	Relative spread of grout for a rectangular channel
I_{max}	Maximum spread of grout
P_0	Pumping pressure
P_I	Ground water pressure inside the fractures
ΔP	Pressure difference
R	Radius of pipe
r	Radius of the spread of grout
Re	Reynolds number
Sen	Saint-Venant number
t	Actual grouting time
t_0	Characteristic grouting time
t_D	Relative grouting time
v	Mean velocity at the grout front
v_{pipe}	Mean velocity at the grout front for flow in a circular pipe
$v_{channel}$	Mean velocity at the grout front for flow in a rectangular channel
v_{radial}	Mean velocity at the grout front for radial flow between parallel disks
Z	Half of the solid core/plug thickness

Greek symbols

ξ	Relative plug thickness
ξ_{pipe}	Relative plug thickness for a pipe
$\xi_{channel}$	Relative plug thickness for a rectangular channel
$\dot{\gamma}$	Shear rate
$\dot{\gamma}_W$	Shear rate at wall
$\dot{\gamma}^*$	Non-dimensional shear rate
τ	Shear stress
τ_W	Wall shear stress
τ_0	Yield stress
μ_B	Bingham plastic viscosity

Table of Contents

1 Introduction

1.1 Current grouting practice

Grouting is performed by injecting fluids inside rock fractures, as shown in Figure 1, with an aim to make the formation stronger, stiffer and less permeable, in order to reduce the lowering of the ground water table. Cement based suspensions are often used as grouting material due to their wide availability and relatively low cost. The grouting design used in practice is mainly based on empirical knowledge and measurement of the grout volume and pressure, in combination with an estimation of the yield stress of the grout used (Lombardi 1985). The rheological properties and selection of the grout mix are considered to be important parameters for designing the grouting work. The selection of grout mix is also mainly based on experience; a stable grout mix was suggested by Lombardi and Deere (1993), i.e., a grout without excessive separation between cement and water.

In recent decades, a grouting design approach based on the penetration length for cementitious grout in rock fractures and the characteristic grouting time has been developed. A significant contribution to the theoretical development of Bingham flow was presented by Gustafson and Claesson (2005) and Gustafson and Stille (2005) and subsequently by El Tani (2012) and finally again by Gustafson et al. (2013). In the first paper, the expression 'characteristic time' was defined and dimensionless curves for relative penetration as a function of relative time were presented. This represented a major breakthrough in the development of analytical solutions for grouting, governing factors and time as an important criterion in grouting practice. Subsequently, the mathematical expressions from Gustafson and Claesson (2005) were simplified by Gustafson and Stille (2005) in order to arrive at useful tools for practical implementation.

These tools are sometimes termed 'RTGC – Real Time Grouting Control'. RTGC relies upon knowledge of the yield stress and viscosity, in addition to their change with time (Kobayashi et al. 2008) and the characteristic grouting time, t_0 , defined as

$$t_0 = \frac{6\mu_g \Delta P}{(\tau_0)^2} \tag{1}$$

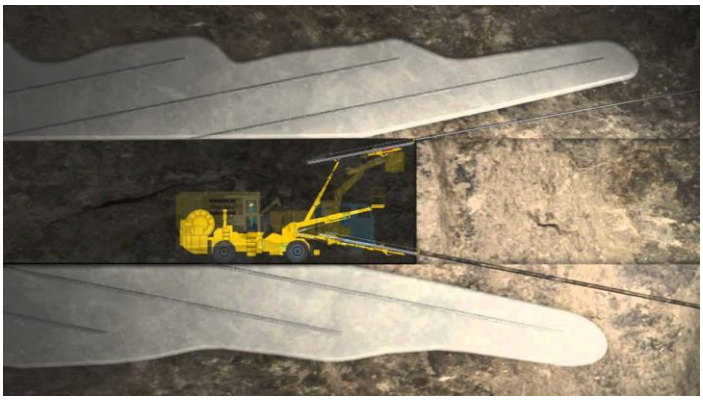

Figure 1 Grouting of boreholes (www.atlascopco.se)

where μ_g is the plastic viscosity, τ_0 is the yield stress and ΔP is the pressure difference between the grout front and the borehole. Therefore, based on the knowledge of these parameters, a stipulated grouting time can be decided, provided that the yield stress and viscosity can be monitored, preferably in real time.

The need of an instrument capable of determining the rheological properties continuously in-line, i.e., during grouting, has been emphasized for many years by different authors, e.g. Barnes et al. (1989); Håkansson (1993); Banfill (2006). However, although the rheological properties of cement based grouts play a fundamental role in grouting design, no method is yet available to measure these properties in-line during field operations. Commercial grouting rigs used today are capable of measuring the pressure, grout flow and time during grouting. However, the rheological properties of the grout used are still measured off-line in a laboratory, and the results are often lacking in reliability and accuracy.

Despite the importance of yield stress as a parameter for designing the spread of grout, there is no standard method to determine the yield stress. The most common technique is to measure the shear stress vs shear rate flow curve and extrapolate to the yield stress at zero shear rate. However, a very accurate measurement is required at low shear rates (Liddel and Boger 1996), and this is often difficult to achieve due to slip at the wall of the measuring device. The vane method offers the superiority of avoiding a slip layer at the wall; however, it has to be operated at low rotating speed to eliminate the effect of secondary flow between the blades (Nguyen and Boger 1983). Due to thixotropy, the yield stress of cement grout also depends on the applied shear history and provides different results depending on the measuring protocol, measurement geometry and other conditions (Barnes and Nguyen 2001; Nguyen et al. 2006). Even though these issues are well known, engineers often have problems defining the yield stress as a constant material property.

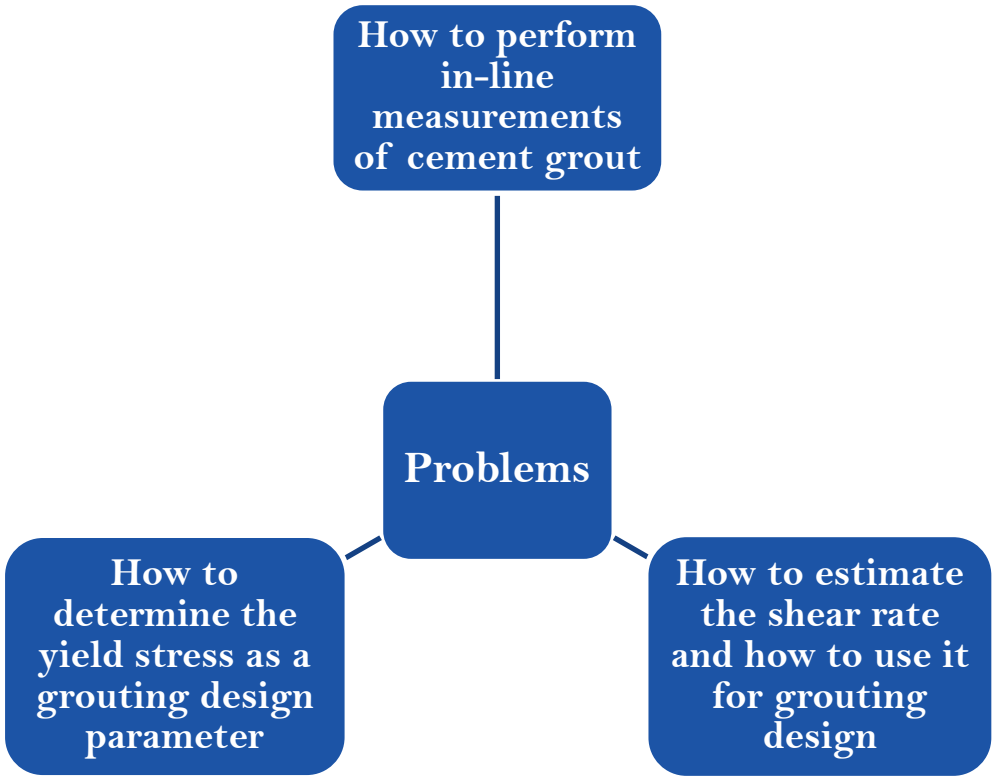

Figure 2 Areas of investigation of this work

In order to solve this issue, two yield stresses, static and dynamic yield stress, were introduced (James et al. 1987; Håkansson 1993) and, to use the corresponding yield stress as a design value, the shear rate at the grout front inside the fracture has to be estimated. Even though closed form solutions are available to estimate the shear rate for Bingham flow in one dimensional geometry, i.e., a circular pipe and rectangular channel, a numerical approach must be used for a two dimensional geometry.

The areas of investigation of this work are shown in Figure 2. The purpose of the work is two folded; firstly to investigate the feasibility of using an ultrasound based in-line rheological properties measurement technique for cement grout, known as Ultrasound Velocity Profiling combined with Pressure Difference (UVP+PD). The second phase involves the investigation of the 'design value' of the yield stress of cement grout with respect to different shear histories and estimation of shear rate using the analytical approach for a one dimensional and a two dimensional geometry. This work introduces a state of the art in-line rheological properties measurement technique for grouting applications and combines the measurements with grouting design theories. This work should therefore, be seen as an effort to bridge the gap between the novel grouting design theories and the UVP+PD measurement technique.

1.2 Previous studies

Research on grouting has been continuous in Sweden for the last 30 years. However, implementation in grouting practice in the field is still lacking. The flow of grouts in jointed hard rock assuming a channel network was simulated by Hässler et al. (1992). The hydration of cement grout and the inclination of the channel network were taken into account, and a significant difference in penetration was shown to be due to the time dependent properties of the cement grout. Rheological properties of cement grouts were measured by Håkansson et al. (1992) using different laboratory and field measurement techniques. It was shown that the determined yield stress and viscosity of the grouts differ significantly depending on the measuring technique. The instruments used in the field were rather simple, and the laboratory based instruments were lacking in reliability and robustness. Furthermore, different rheological models yield different values for the rheological properties. A field instrument, the 'raise pipe', was developed to determine the yield stress, which can be used in combination with the Marsh cone to also determine the viscosity of the grout. The influence of the cement, additives and plasticizers on the rheological properties of cement grout was investigated. It was concluded that flow properties can be improved significantly by using plasticizers in a cement grout (Håkansson et al. 1992).

To determine the yield stress of grout, the cohesion plate was introduced by Lombardi (1985). It consists of a plate that is dipped into the grout and, by measuring the weight of the plate before and after, the weight of the grout that adheres to the plate is determined. The Marsh cone measures the apparent viscosity, i.e. the flow time is dependent on a combined effect of all rheological properties of the grout. In addition, two parameters, the plastic viscosity and the yield stress, must be known in order to describe the rheological behavior of a fluid, which means that two separate measurements must be made. To relate the flow properties to the yield shear stress, Lombardi (1985) developed relationships for the Marsh cone and the cohesion plate. It was proposed that the Marsh cone should be combined with the cohesion plate to separately determine the viscosity and the yield stress. Håkansson (1993) established a theoretical model for the relationship between plastic viscosity, yield stress and Marsh cone flow time. This means that, by measuring the yield stress with another method, the Marsh cone flow time can also be used to determine the plastic viscosity. Roussel and LeRoy (2005) developed a method to determine the yield stress using two flow cones. However, limitations regarding the flow cone remain, e.g. if the fluid viscosity is too low, there is no linear relation between viscosity and flow time; and, if the pressure gradient is not sufficient to overcome the yield stress of the fluid, no flow will occur. A simple method, the 'yield stick', to determine the yield stress of grout was introduced by Axelsson et al. (2006). The stick is allowed to sink into the grout and, from the length of the stick inside the grout, the yield stress is calculated by equilibrium of the forces. However, this method does not

provide further information, i.e. change due to the thixotropic behavior, hydration etc. of the grout.

In-line ultrasound based rheometry, e.g., Ultrasound Velocity Profiling combined with Pressure Difference (UVP+PD) is a promising method to determine the rheological properties directly in-line in flowing conditions. This method has been successfully used to determine the rheological properties of food suspensions, mine tailings and paper pulp (Birkhofer 2007; Wiklund et al. 2006; Wiklund et al. 2007; Kotze' et al. 2008). Real-time visualization of the velocity profiles directly in-line during the ongoing process and the non-invasive measurement capabilities make UVP an important tool for engineering and research applications. The fact that most industrial fluids are opaque makes UVP the only available tool for flow measurements and visualization, as other techniques are usually based on visible light such as Laser Doppler Anometry (LDA). However, this method has never been used for cement suspensions.

The estimation of grout spread assuming the grout as a Bingham material for a radial disk flow was performed by Gustafsson and Stille (2005). The estimation of grout spread was shown as a relative distance to the maximum spread. However, an estimation of shear rate was lacking. This was due to the fact that the estimation of shear rate requires estimation of the plug thickness, which was not available. Since the grout is a thixotropic material, the determination of yield stress and viscosity relies on the applied shear rate range and, in order to achieve a realistic result in comparison to the practical applications, the estimation of the shear rate is necessary.

Therefore, judging from the works mentioned above, there is a gap regarding continuous in-line measurement of the rheological properties of grout and application of this information in practice.

1.3 Objectives

The main objectives of this study were the following

1. To verify the feasibility of the ultrasound velocity profiling combined with the pressure difference (UVP+PD) method for determining the rheological properties of grout.

2. To measure the yield stress using different measurement techniques, i.e., conventional off-line rotational rheometry, ultrasound based in-line measurement technique and defining the criteria for 'design value' of yield stress for grouting applications.

3. To estimate the plug thickness, velocity and shear rate of cement grout using an analytical approach for one dimensional and two dimensional geometry for a constant pressure.

4. To develop a non-dimensional nomogram in order to facilitate the design with respect to the velocity and shear rate of the grout inside the rock fractures.

In order to achieve the main objectives of the work, secondary objectives were implemented at different stages of the project. The secondary objectives were the following

1. Measurement of the velocity profiles of cement based grouts for different water to cement ratios directly in-line using customized flow loops.

2. Determination of the change of the rheological properties of cement grout with time using the Bingham model, Herschel-Bulkley model and non model approach.

3. Determination of the volumetric flow rate directly in-line by the UVP+PD method and comparison of the results with a flow meter for field use (LOGAC™) and a conventional electromagnetic flow meter.

1.4 Organization of the thesis

This thesis starts with an introduction describing the necessity of determining the rheological properties of cement grout directly in-line. It furthermore indicates the gap of knowledge regarding the 'design value' of yield stress and its determination with respect to the prevailing shear rate. The introduction continues with a description of previous research studies on cement based grouts, concerning models of the penetration of cement grout in rock fractures, influence of the rheological properties and measuring techniques.

The theories concerning the flow of Bingham fluids, rheology of cement grout and different measurement techniques are presented in chapter two. Measurement techniques consist of different laboratory and field techniques, and their limitations are discussed.

The working principles of the UVP+PD method are described in chapter three. The methodology consists of two parts, Ultrasound Velocity Profiling (UVP) and UVP combined with the Pressure Difference (PD).

The experimental set-up and different equipment used are presented in chapter four.

The results are shown and discussed in chapter five. Conclusions follow in chapter six.

This research work resulted in several appended papers, which are briefly described below.

Paper I: Wiklund, J., Rahman, M., Håkansson, U., 2012. In-line rheometry of micro cement based grouts - A promising new industrial application of the ultrasound based UVP+PD method. *Applied Rheology 22, 42783.*

In this paper, rheological properties determined by the UVP+PD method are presented and compared with off-line measurements. The rheological properties were determined using rheological models, e.g. Bingham and Herschel Bulkley. In addition, a non-model approach, the gradient method, was used. This is the first time the UVP+PD method was used for cement based grouts in field like conditions. It was possible to measure the velocity profiles up to the center of the pipe for w/c ratios of 0.6 and 0.8, which is a prerequisite for determining the rheological properties using the UVP+PD method. However, the results showed the need for an improved transducer design capable of generating sufficient energy for accurate measurements of the velocity profiles. Off-line measurements were made and found to be in good agreement with the in-line results. Volumetric flow rates were determined and subsequently compared with the commercial flow meter LOGAC™ device. The UVP+PD method was found to be a promising tool for determining the rheological properties of cement grout in-line, under field like conditions, and to be capable of performing an accurate measurement and visualization of the flow rate.

Paper II: Rahman, M., Håkansson, U., Wiklund, J., 2015. In-line rheological measurements of cement grouts: Effects of water/cement ratio and hydration. *Tunnelling and Underground Space Technology 45 (34-42).*

The work reported in this paper investigated the feasibility of the UVP+PD method for determining the change of the yield stress and viscosity of cement grout with respect to concentration and time. Yield stress and viscosity were determined using the Bingham and Herschel Bulkley rheological models. In addition, a non-model approach, the gradient method and tube viscometry concept, was used and subsequently compared with the results obtained by the rheological model fitting procedure. A new non-invasive sensor unit was used and found to be capable of generating sufficient energy to measure the instantaneous velocity profiles beyond the center of the pipe for w/c ratios down to 0.6. A laboratory based flow loop was used to achieve a stable flow rate. The volumetric flow rate was determined by integrating the velocity profiles and was subsequently compared with the LOGAC™ commercial flow meter and an electromagnetic flow meter. The UVP+PD method was capable of determining the change of the rheological properties of cement grout with respect to concentration and time directly in-line. In addition, it was found to be an effective tool for visualization and accurate flow measurement.

Paper III: Rahman, M., Wiklund, J., Håkansson, U., 2015. Yield stress of cement grout. *Submitted to the journal Tunnelling and Underground Space Technology.*

In this paper, the yield stress of cement grout was measured using different measurement techniques and the results were compared. Stress ramp, constant shear rate, stress relaxation and creep tests were performed using a conventional rotational rheometer. In addition, direct measurement of yield stress was made using the in-line ultrasound based 'UVP+PD' method. The tests were done with respect to the shear history, i.e., aging and structural breakdown of the particle bonding in order to define the different states of cement grout. A water to cement ratio of 0.7 was used as a reference grout. Two states of yield stress, i.e. static and dynamic yield stress, were defined depending on the applied shear rate on grout and it was concluded that the design value of yield stress should be chosen with respect to the applied shear rate at the grout front during grouting applications.

Paper IV: Rahman, M., Hässler, L., Håkansson, U., 2015. Cement grouting design– a nomogram for velocity, plug thickness and shear rate. *Submitted to the journal Rock Mechanics and Rock Engineering.*

The purpose of this paper was to provide an analytical approach for the determination of velocity, plug thickness and shear rate of cement grout during propagation inside the rock fracture. Comparisons were made of the results for a one dimensional pipe, channel and a two dimensional radial disk geometry. Numerical calculations and a comparison with experimental work were also made in order to verify the analytical results. Further, a non-dimensional nomogram was developed in order to simplify the design with respect to the velocity and shear rate of the grout inside the rock fractures.

Paper V: Rahman, M., Håkansson, U., Wiklund, J., 2012. Grout pump characteristics evaluated with the Ultrasound Velocity profiling. *In: Proceeding of ISRM International Symposium, EUROCK, 28th-30th May 2012, Stockholm.*

In this paper, the Ultrasound Velocity Profiling (UVP) technique was shown to be an effective tool for determining the characteristics of the grout pump. A standard grouting rig, UNIGROUT E22H, and a laboratory based set-up with a progressive cavity type of pump were used, and the instantaneous velocity profiles were measured. A large fluctuation in the velocity was observed due to the piston type of pump used in the grouting rig. A negative velocity was also observed which was due to the backstroke of the piston. This is a unique feature of the UVP that cannot be obtained by other methods. In contrast and as expected, the progressive cavity type pump provided a very stable flow rate. Based on the visualization of the pulsed flow, characteristics of the grout pump can be determined and optimized for practical grouting. In addition, UVP was found capable of making accurate determinations of

the flow rate when it is less than 1 liter/min, which is not possible using commercial flow meters. Since field grouting work is based on empirical methods and the determination of the flow and pressure, a device capable of making accurate measurements of the flow rate would lead to a better determination of the execution time in grouting practice.

2 Background

2.1 Introduction

In this thesis, the rheological properties of cement grout were investigated using different measurement techniques and were combined with state of the art design procedures for the stop criteria of grouting works. Understanding of the rheology of cement grout, principles of measurement techniques and theories concerning the spread of grout were thus of major importance. The fundamentals of the theoretical background are shown in the following sections.

2.2 Rheology of cement grouts

Rheology is the science of deformation and flow of matter. The rheological behavior of cement based grout can be considered complex (Håkansson 1993). The grout is non-Newtonian and, thixotropic and has a yield stress. Further, the hydration of the cement also plays a key role, as the rheological properties change with time. The rheology of cement grout is a factor of prime importance in transporting, pumping, pouring and spreading of the material. In practice, cement grouts with water to cement ratios of 0.6-1.5, consisting of a solid volume concentration of approximately 30%-50%, are used (Rosquoët et al. 2003). In concrete, a complete breakdown is achievable at the end of mixing which is dependent on the aggregate content. In contrast, for cement grouts, due to the absence of aggregate, the surface area of the finer cement particle is higher and the rheology is more complex as a result of the interaction between the suspended particles and the breakdown during shearing. Typical values of the rheological properties of the cement based materials are shown in table 1 (Banfill 2003).

Cement grouts and cement based materials are subject to hydration, and the rheological properties change accordingly. As observed by Håkansson (1993) and summarized by Banfill (2006) and Sant et al. (2008), hydration proceeds in several stages. The first stage involves a rapid reaction between the anhydrous minerals and water, resulting in a wetting peak. Subsequently, a slow reaction for two or more hours known as the dormant period is followed by an accelerated stage responsible for interlocking. Finally, the fourth stage involves the

deceleration process. As a consequence, the apparent viscosity of the cement based materials will change in accordance with the hydration process.

Rheological properties of cement based materials are often expressed by a curve fitting constitutive model to the shear stress vs. shear rate data. Different rheological behaviors are shown in Figure 3. Newtonian fluids do not have a yield stress and have a constant viscosity. Pseudo plastic fluids do not have a yield stress however show a shear thinning behavior with an increased shear rate and can be represented by using a power law model. Bingham fluids have a yield stress and a constant viscosity. Yield pseudo plastic fluids have a yield stress and show a shear thinning behavior with an increased shear rate.

Table 1 Typical values of the rheological properties of cement based material, Banfill (2003)

Material	Cement paste, Grout	Mortar	Flowing concrete	Self-compacting Concrete	Concrete
Yield stress N/m^2	10-100	80-400	400	50-200	500-2000
Plastic viscosity Pa.s	0.01-1	1-3	20	20-100	50-100
Structural Breakdown	Significant	Slight	None	None	None

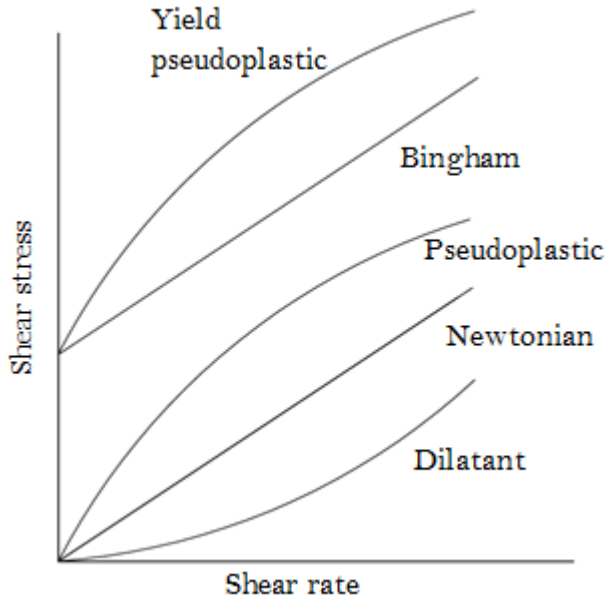

Figure 3 Rheological behavior of Newtonian and non-Newtonian fluids

Yield pseudo plastic behavior can be represented by using the Herschel Bulkley (H-B) model. Dilatant fluids show a shear thickening behavior with an increased shear rate. The Bingham model is widely used owing to its simplicity and the linear relationship between shear stress and shear rate. However, the rheological behavior of dense cement based materials can be better represented by the Herschel-Bulkley model since it can model the shear thinning behavior that is observed (De Larrard et al. 1998). The Bingham model and the Herschel-Bulkley model are shown as:

$$\text{Bingham}: \quad \tau = \tau_0 + \mu_B \dot{\gamma} \tag{2}$$

$$\text{Herschel-Bulkley}: \quad \tau = \tau_0 + k \dot{\gamma}^n \tag{3}$$

where τ is the shear stress, τ_0 is the yield stress, μ_B is the Bingham viscosity, k is the consistency index and n is the flow index. As can be seen, both of the models include a yield stress. In the Bingham model, the viscosity is expressed by a linear relationship with the shear rate while, in the Herschel-Bulkley model, the shear thinning behavior is represented by the flow index, n. The flow of material is resisted by viscosity, and it is defined as the relationship between the shear rate and the stress applied to the material. A variation in the apparent viscosity can be observed with changes of temperature.

The, determination of the plastic viscosity and the consistency index, k, by the Bingham and Herschel-Bulkly models might also yield different results for the same sample due to the shear rate range of the mathematical fitting. As shown by e.g. Nehdi and Rahman (2004), the

Bingham model will always yield a higher viscosity than other nonlinear rheological models, e.g. the Herschel Bulkley model.

2.2.1 Yield stress

The yield stress is the material property that denotes the transition between solid like and fluid like behavior. Consequently, it is the minimum stress that makes the fluid flow like a viscous material. Inter-particle forces between the solids in a suspension result in a yield stress that must be overcome to start the flow, and an applied stress that is lower than the yield stress will result in a deformation like a solid instead of flowing. The existence of a yield stress has been questioned by some authors, e.g. Barnes and Walters (1985), due to the fact that, given accurate measurements at very low shear rates, no yield stress exists.

The historical concept of yield stress was summarized by Barnes (1999), and the argument on the existence of yield stress was concluded by the fact that it is acceptable to describe the material behavior with a yield stress over a limited shear rate range; however, this is represented by limited data.

The problem associated with the yield stress is the difficulty in determining it. Theoretically, at the yield stress, the apparent viscosity of the material changes from a finite value to infinity; therefore, an infinite duration of a test is required (Barnes 1997; Barnes 1999). Yield stress fluids show an elastic behavior prior to reaching the yield stress. Prior to reaching the yield stress, the material behavior changes to non-linearity from linearity and a residual stress is followed after the peak stress. Therefore, defining the yield stress is also a point of debate and a range of yield stress can be used for practical applications (James et al. 1987; Mujumdar et al. 2002).

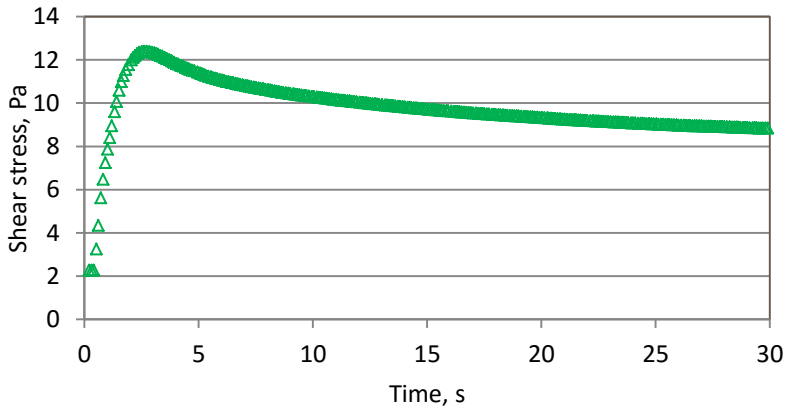

Figure 4 Measurement of yield stress of cement grout

In this work and for grouting purposes, yield stress is seen as an engineering reality, and this fact was also used in other works, as long as the application generates the same range of shear rates that have been measured (Hartnett and Hu 1989; Schurz 1990). An example of the measurement is shown in Figure 4 to illustrate the yield stress of grout, and the above mentioned phenomena are visible there. The yield stress is normally measured using different types of viscometers, e.g. rotational, cone and plate, tube etc. As shown by Mannheimer (1991), the wall slip effect is a major problem when measuring the yield stress of cement slurries, especially at lower shear rates.

Constitutive equations and rheological models are used to extrapolate the resulting fitted curve to zero shear rates, since it is not possible to obtain the shear stress at zero shear rate using conventional rotational rheometers. When using analytical models to determine the yield stress of the grout, it should be noted that different models will yield different results depending on the shear history of the material (Yahia and Khayat 2003).

2.2.2 Thixotropy

When the fluid is thixotropic, the yield stress becomes a function of build-up (aging) and break-down (shear rejuvenation) of the material during shearing (Moller et al. 2009a). In order to properly evaluate rheometric data, one needs to distinguish between two types of yield stress fluids, thixotropic and non-thixotropic, or "simple". A thixotropic fluid is one for which the rheological behavior is dependent on the shear history of the sample. The rheological behavior is influenced by the competition between a spontaneous build-up of some microstructure at rest ("aging") and its break-down by flow ("shear rejuvenation") (Bonn et al. 2004). The yielding of material is governed by the competition between aging and shear rejuvenation, which eventually leads to the bifurcation behavior of viscosity. This implies that, at an applied stress higher than the yield stress, the viscosity is decreased and reaches a finite value with time. However, at an applied stress lower than the yield stress, the viscosity increases with time (Coussot et al. 2002a; Coussot et al. 2002b).

Thixotropy can also be explained by the fact that the apparent viscosity of a material increases when it is at rest and decreases with an increase in the shear stress as shown in Figure 5 for cement grout. The history and the definitions of thixotropy have been summarized by Barnes (1997). What is implied is a decrease in shear stress at constant shear rate or a decrease in shear rate at constant shear stress. Moreover, the phenomenon of thixotropy can be observed by a hysteresis loop in the shear stress-shear rate curve of a cement suspension. Since the flocculated structures are broken down, the down curve will show a decrease in shear stress at the same shear rate compared to the up curve. The true thixotropic behavior of cement paste, e.g. coagulation, dispersion and re-coagulation of the

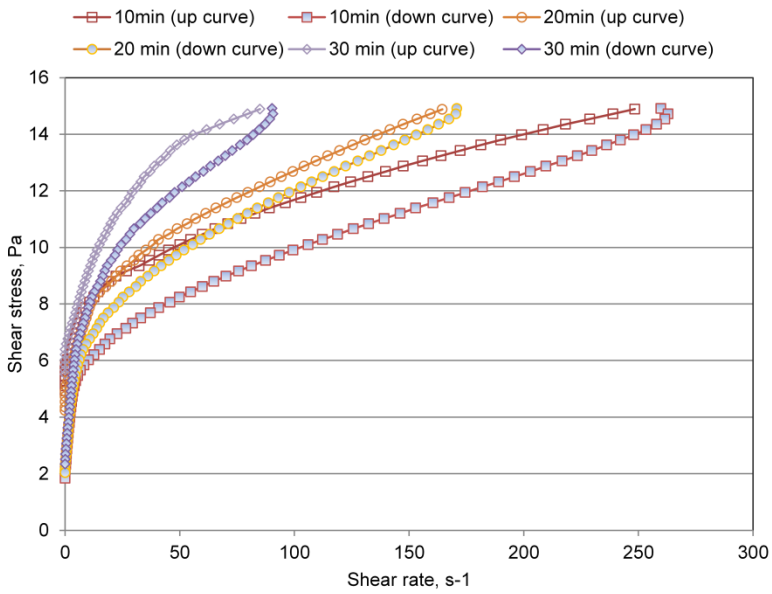

Figure 5 Thixotropic behavior of cement grout

cement particles, plays a major role in generating the time dependent behavior. The structural breakdown refers to the process of breaking linkages between the cement particles. Based on this assumption, a material model (PFI – Particle Flow Interaction model) to simulate the rheological behavior of cement paste was proposed by Wallevik (2009). The coagulation process is due to the potential energy of the particles, which 'glues' them together when they come into contact with each other for a certain duration of time.

However, this coagulation can be referred as 'reversible' and 'irreversible' depending on the breakage of the linkage of the particles. The time dependent shear response of cement paste with a low water to cement ratio was shown by Sant et al. (2008). At an early stage, the shear stress was observed to reach equilibrium after a peak shear stress. However, at a later stage, the shear stress increased rapidly and the measured shear stress exhibited a saw-tooth response. This can be explained by the continuous loss and recovery of inter-particle forces under the applied stress.

Besides in cement, thixotropic behavior was observed in Bauxite residue (Nguyen and Boger 1985). The yield stress decreased over time and an equilibrium state was achieved while shearing for a longer period. In addition, the recovery time was very high when the suspension was at rest, which showed an irreversible thixotropic structure associated with the red mud suspension. This was explained by the fact that two types of bonds were present in the system, the inter-particle bond and the inter-aggregate bond. While the suspension was under shear, an applied stress higher than the yield stress broke the inter-aggregate bonds in an irreversible manner and the inter-particle bonds were broken in a reversible

manner. An equilibrium of yield stress over a longer shearing period indicated that the aggregate structure cannot be destroyed by prolonged shearing but will rest at a certain level. As summarized by Banfill (2006), the practical significance of the thixotropy in cement systems lies in the rapid structural build-up that reduces the pressure exerted by self-compacting concrete in formwork. In addition, the rapid stiffening of sprayed concrete prevents it from slumping before setting. Further, thixotropic slurries have been found problematic in connection with flow in pipes. When flowing through a pipe, the liquid near the pipe wall will be highly sheared and will be subjected to rapid and prolonged breakdown. As a result, a lower viscosity will prevail near the pipe wall. At the center of the pipe, however, the shearing will be lower; hence a plug would be present.

2.3 Measurement techniques

Measurements of the rheological properties of cement based grouts are made in the laboratory and in the field. Instruments that are used in the laboratory are not robust, and instruments that are used in the field are rather primitive and their results might be unreliable and difficult to reproduce (Håkansson and Rahman 2009). Depending on the procedure of rheological measurements, they can be defined as off-line and in-line. Off-line measurements are performed in the laboratory, which implies that there is a stop during the process conditions, and the shear history and results cannot be readily comparable. In contrast to the off-line measurements, in-line measurements (e.g. UVP+PD) are performed in the process itself and the results are comparable to the prevailing conditions.

2.3.1 Off-line measurement techniques

Off-line measurements are made using different types of rheometers. Rheological properties can be measured by rotational rheometers using indirect and direct techniques. As mentioned by Nguyen and Boger (1983), indirect methods can be referred to as the direct extrapolation of the rheological shear rate-shear stress data, i.e. the flow curves assuming different rheological models. Direct methods are for example the shear stress relaxation method and the shear vane method.

When measuring the rheological properties of cement grout using a rotational rheometer, the concentric cylinder geometry is often used. The advantage is that this geometry requires only a small sample that can be measured for a long period of time. However, a measurement with the concentric cylinder geometry should be performed with care since the wall slip phenomenon is inevitable when measuring a shear thinning thixotropic suspension (Barnes 1995). The wall slip occurs due to the displacement of the disperse phase (concentrated suspension) away from the solid boundary, leaving a low viscous layer near the smooth wall.

To eliminate the wall slip effect, Nguyen and Boger (1983) introduced the vane method. The complexity associated with the measurement at low shear rates and the model fitted parameters was discussed. The significance of measuring the shear stress-shear rate data by a direct method was stressed. The measurement with the vane geometry is independent of the vane dimension and size and was shown to be more accurate for highly concentrated thixotropic suspensions. Further work by Nguyen and Boger (1987) showed that, when measuring a concentrated suspension of thixotropic material using the concentric cylinder, the sample might be partially sheared due to the yield stress.

Creep tests are done to investigate the material response under an imposed stress. Creep tests can be performed using a concentric cylinder, vane or parallel plate geometry. However, for cement grouts, a concentric cylinder or vane geometry is used due to the low viscosity of the material. By performing creep tests at stresses below and above the yield stress, the change of the material response from viscoelastic solid to viscous liquid can be observed (Struble and Schultz 1993).

A problem associated with the measurement of rheological properties of non-Newtonian suspensions using rheometer is that the reproducibility of the results is fairly low and, due to a different shear history of the sample, they cannot be compared to the industrial applications (Nguyen et al. 2006). In addition, significant errors in determination of the rheological properties can occur if the appropriate equations for the calculations are not used or misunderstood (Wallevik et al. 2015). Comparisons of the rheological properties, measured by different rheometers from a number of laboratories, were made for concrete and a discrepancy in the results was found (Ferraris et al. 2001). The measured rheological properties are dependent on the rheometer used. Therefore, a standard reference material (SRM) was developed for cement paste and mortars (Ferraris et al. 2014). However, such a reference for cement grout is lacking.

Tube viscometers are the most commonly used instruments for measuring viscosity because of their low cost and simplicity. When a fluid is driven by pressure through a pipe, the velocity is at its maximum at the center, which implies that the velocity gradient or shear rate is at its maximum at the pipe wall and zero at the center. The wall shear stress is obtained from the pressure difference over a known distance. The shear rate is determined assuming a Newtonian fluid, and a correction factor, e.g. Rabinowitsch–Mooney, is applied to determine the shear rate for a non-Newtonian fluid. As a result, the wall shear stress vs. wall shear rate curve is obtained, provided that pipes with different diameters with the same length/radius ratio are used. The wall slip phenomenon is evident for cement grout when tube viscometers are used. A cement layer is depleted at the pipe wall, and the smooth surface provides a lower viscosity of the grout. The wall shear rate should therefore be corrected because of the slip.

More detail on tube viscometry can be found in Mannheimer (1991) and Barnes (1999).

2.3.2 In-line measurement techniques

In-line measurements are made under process conditions in the process line and are usually non-invasive. However, due to the difficult process condition requirements, e.g., high temperature, and harsh field conditions, in-line rheological properties measurement systems are still under development and are mainly used for research purposes. The examples are, e.g., the optical point-wise laser Doppler anemometry (LDA) technique, the nuclear magnetic resonance imaging (NMRI) method, based on the paramagnetic properties of the nuclei, and the ultrasound velocity profiling (UVP) technique, which employs the successive emissions of ultrasound pulses and estimation of velocity in concentrated suspensions for in-line measurements of the rheological properties (Takeda 1986; Wiklund et al. 2006). For mineral slurries, a rheometer was used in a customized flow loop in process conditions for on-line measurements of the rheological properties and good agreement was reported with a commercial off-line rheometer (Akroyd and Nguyen 2003).

In this work, the ultrasound based UVP+PD method was used to perform the flow measurement, flow visualization and in-line measurement of cement grout.

2.4 Ultrasound Velocity Profiling (UVP)

Ultrasound Velocity Profiling (UVP) is a technique to measure the instantaneous velocity profiles of opaque fluids inside a pipe. The technique was originally developed in medicine to measure blood flow and was subsequently extended by Takeda (1986) for application in fields of engineering. The working principle is based on the emission of pulsed ultrasound bursts and echo reception along the beam axis. This technique determines the relative time lags of the echoes received between successive emitted pulses. The time lags are related to the speed of the moving fluid at a certain position. As a consequence, the complete velocity profile as a function of distance (or pipe diameter) can be measured.

2.4.1 UVP+PD method

The UVP+PD is based on the pipe viscometry concept. The UVP+PD methodology is basically a tube viscometer with multi-point velocity measurements. The limitation of the capillary viscometer instrument is that it only provides single point data corresponding to a specific shear rate, hence limiting its use for non-Newtonian fluids. In contrast, the UVP+PD method allows real-time measurements of radial velocity profiles and hence complete flow curves. From the data derived, rheological properties such as viscosity and yield stress can be determined directly in-line.

The potential of this method for measuring the rheological properties of cement grouts was discussed by Håkansson and Rahman (2009) and the feasibility of this method was investigated by Håkansson et al. (2012) and, Rahman et al. (2015). It was subsequently found that the UVP technique itself can be a very good method for evaluating the grout pump characteristics with respect to pulsation (Rahman et al. 2012). The UVP+PD technique has also been successfully used in various other industrial suspensions, such as food, paper pulp and mine tailings, e.g. (Wiklund et al. 2006; Birkhofer 2007; Wiklund et al. 2007; Kotzé et al. 2008).

The key advantage of the UVP+PD method is the determination of the true rheological properties using the non-model approach. The shear rate is calculated from the gradient of the velocity profiles, and the yield stress is determined from the plug radius. However, the non-model approach is sensitive to noise and requires an accurate measurement of the velocity profiles. The procedure of the determination of rheological properties by the UVP+PD method is shown in Figure 6.

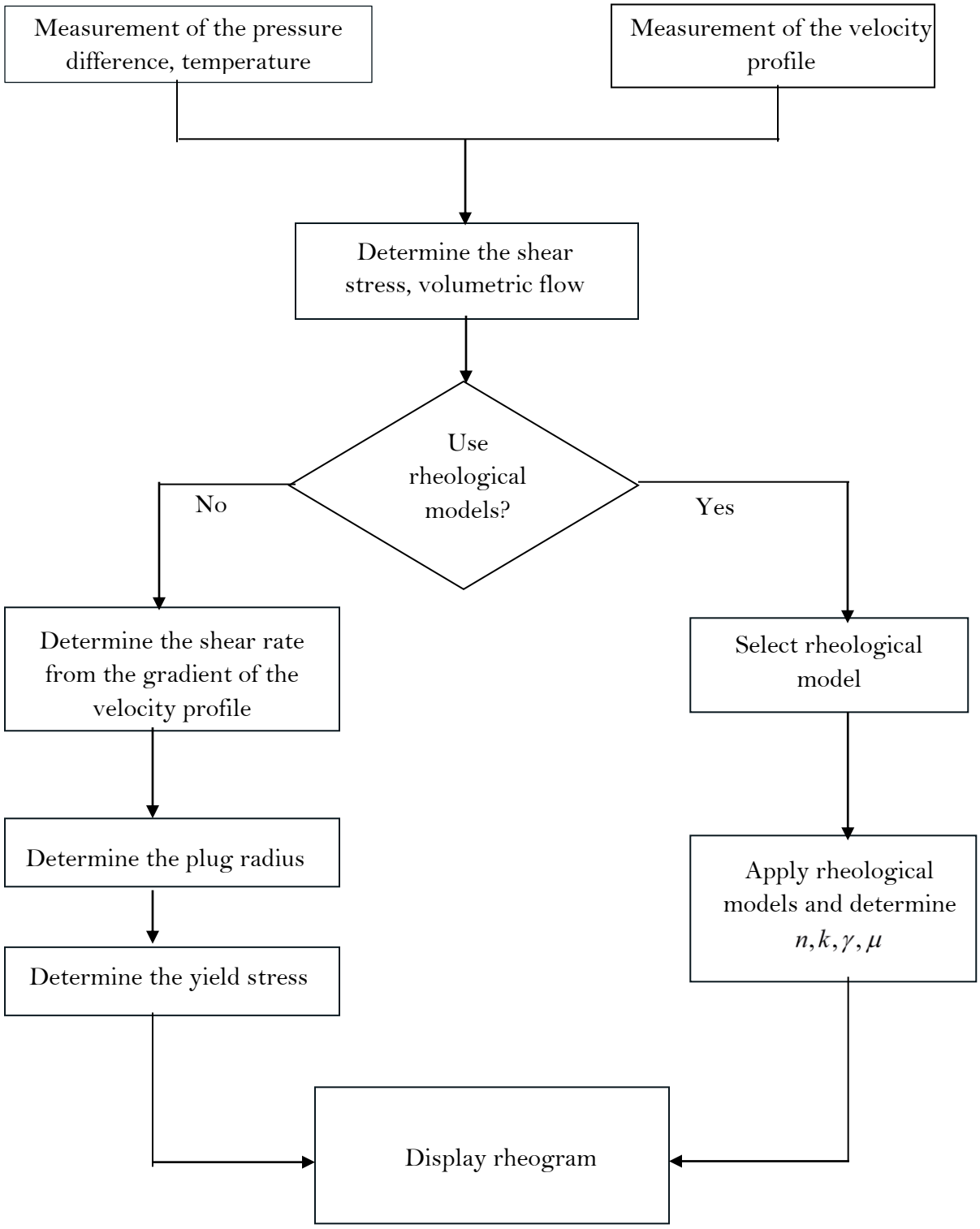

Figure 6 Rheological properties determination flow chart using the UVP+PD method

2.5 Flow of Bingham fluids

2.5.1 Theoretical background

The flow of fluids can be described by two fundamental equations of fluid mechanics, equation of continuity and the equation of motion. A schematic illustration of fluid flow inside a one dimensional channel and a two dimensional radial disk are shown in Figure 7 and Figure 8 respectively.

Based on the cylindrical coordinates, the equation of continuity can be shown as (Bird et al. 1960)

$$\frac{\partial \rho}{\partial t}+\frac{1}{r}\frac{\partial(\rho r v_r)}{\partial r}+\frac{1}{r}\frac{\partial(\rho v_\theta)}{\partial \theta}+\frac{\partial(\rho v_x)}{\partial x}=0 \tag{4}$$

where v_r, v_θ and v_x are the velocity components in the radial, tangential and axial directions, respectively. The basic assumptions of the flow are that this is an incompressible fluid, fully developed, steady laminar flow, flows only in the x and r direction for the pipe and radial disk, respectively, and there is no slip at the wall. Therefore, the equation of continuity for a pipe and radial disk can be shown as equations 5 and 6 respectively

$$\frac{\partial v_x}{\partial x}=0 \tag{5}$$

$$\frac{1}{r}\frac{\partial(r v_r)}{\partial r}=0 \tag{6}$$

The equation of motion for the x component for 1D pipe can be shown as equation 7.

$$\rho\left(\frac{\partial v_x}{\partial t}+v_z\frac{\partial v_x}{\partial z}+\frac{v_\theta}{z}\frac{\partial v_x}{\partial \theta}+v_x\frac{\partial v_x}{\partial x}\right)=-\frac{\partial P}{\partial x}-\left(\frac{1}{z}\frac{\partial(z\tau_{xz})}{\partial z}+\frac{1}{z}\frac{\partial \tau_{\theta x}}{\partial \theta}+\frac{\partial \tau_{xx}}{\partial x}\right)+\rho g_x \tag{7}$$

Due to the incompressibility of the fluid, $\frac{\partial v_z}{\partial t}=0$ and that there is no variation of velocity along the x axis would lead to, $\frac{\partial v_x}{\partial x}=0$ and $\frac{\partial \tau_{xx}}{\partial x}=0$. Due to the symmetry, $\frac{\partial \tau_{\theta x}}{\partial \theta}=0$. Assuming the flow in a horizontal direction, $\rho g_x=0$ and assuming there is flow in only in the x direction, $v_\theta=0, v_z=0$.

Therefore, the equation of motion for 1D flow is reduced and, after further integration with respect to z, can be shown in equation 8 for a pipe.

$$\tau_{xz} = \frac{\partial P}{\partial x}\frac{z}{2} \tag{8}$$

Considering the pressure difference between the start and end point of the 1D flow, $(p_0 - p_I) = \Delta P$, the pressure gradient can be simplified and shown as $\frac{\partial P}{\partial x} = -\frac{\Delta P}{I}$, where I is the distance between the pressure measurements. The shear stress distribution at any cross section of a pipe or channel over a distance I can be derived as linear and shown as

$$\tau = \frac{z\Delta P}{2I} \tag{9}$$

Since the shear stress distribution at any cross section is linear, the shear stress at the wall can be shown as

$$\tau_W = \frac{b\Delta P}{4I} \tag{10}$$

In order to initiate a flow of cement grout, the yield stress must be exceeded. Therefore, at a cross section, where the shear stress is less than the yield stress, a plug is formed which flows as a solid core. Due to a linear distribution of the shear stress at a section, the yield stress can be shown as

$$\tau_0 = \frac{Z\Delta P}{2I} \tag{11}$$

where Z is half of the plug thickness. The relative plug thickness is defined as the ratio of the solid core and the distance of the wall. For a one dimensional geometry, the relative plug thickness can be shown as

$$\xi_{pipe} = \xi_{channel} = \frac{2Z}{b} = \frac{\tau_0}{\tau_W} \tag{12}$$

As shown in Figure 7, the thickness of the channel is b and the thickness of the stiff plug is 2Z. When the maximum penetration for a particular applied pressure is reached, the flow stops and the plug thickness is 2Z=b. The maximum penetration length , $I_{\max}$, can be derived and shown as(Hässler 1991)

$$\mathrm{I}_{\max} = \frac{b\Delta P}{2\tau_0} \tag{13}$$

When a yield stress fluid is flowing in a 1D geometry, the plug thickness can be shown as

$$Z = \tau_0\left(\frac{dP}{dx}\right)^{-1}, Z\langle\frac{b}{2} \tag{14}$$

From equations 10 and 13, the relative penetration I_D can be shown as

$$I_D = \frac{I}{I_{\max}} = \frac{2Z}{b} = \xi \tag{15}$$

The equation of motion, for the r component for 2D radial disk can be shown as equation 16.

$$\rho(\frac{\partial v_r}{\partial t}+v_r\frac{\partial v_r}{\partial r}+\frac{v_\theta}{r}\frac{\partial v_r}{\partial \theta}-\frac{v_\theta^2}{r}+v_z\frac{\partial v_r}{\partial z})=-\frac{\partial P}{\partial r}+(\frac{1}{r}\frac{\partial(r\tau_{rr})}{\partial r}+\frac{1}{r}\frac{\partial(r\tau_{\theta r})}{\partial \theta}-\frac{\tau_{\theta\theta}}{r}+\frac{\partial \tau_{zr}}{\partial z})+\rho g_r \quad (16)$$

Using similar assumptions as in 1D flow, the equation of motion for a 2D circular disk reduces to

$$\frac{\partial P}{\partial r}=\frac{\partial \tau_{zr}}{\partial z} \quad (17)$$

However, for a radial flow, the pressure distribution is nonlinear; therefore, I_D will not be the same as ξ. The shear stress distribution at any cross section of a radial flow is linear and therefore, the plug thickness at a cross section can be defined as

$$\xi_{radial}=\frac{\tau_0}{\tau_W}=\frac{2Z}{b} \quad (18)$$

For simplicity, the Bingham model is widely used for the purpose of designing grouting works. The constitutive relation of the Bingham model can be shown as given in Bird et al. (1960), which is valid when $\tau>\tau_0$

$$\tau=\tau_0+\mu_B\frac{dv}{dx} \quad (19)$$

A constitutive rheological model must be used to obtain the expression of velocity distribution. For the Bingham model, the shear stress and yield stress can be replaced with the plug thickness and, after further integration for a boundary condition of $v=0$ for $Z=R$, the expression of velocity can be obtained, which is well known as the Buckingham-Reiner equation. For a rectangular fracture, it is assumed that all velocities are zero except $v(x)$, which is in the direction of the x axis. In order to derive the expression for velocity, the equation of motion can be simplified and, after further integrations, an expression for the average velocity across the cross section can be derived. For two dimensional flow, the expression for velocity can be developed in the same way as for one dimensional flow, i.e., channel, although, using a constant flow (Bird et al. 1983).

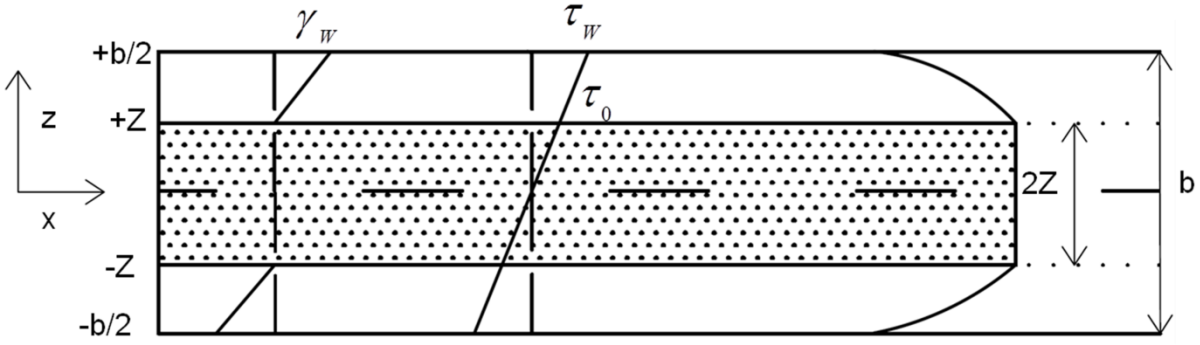

Figure 7 Schematic illustration of Bingham flow in one dimensional geometry

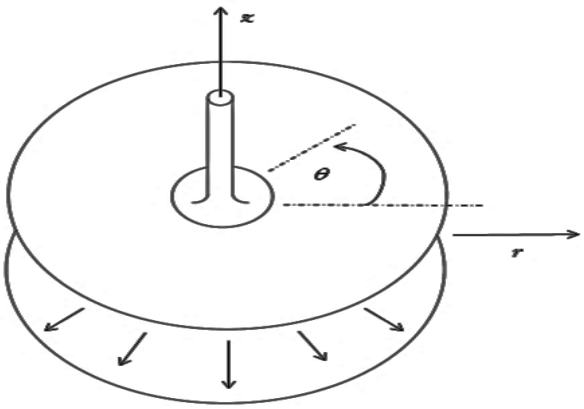

Figure 8 Schematic illustration of Bingham flow in two dimensional radial disk

2.5.2 Estimation of grout spread

Estimations of grout spread in a rock fracture were initiated by Wallner (1976). A numerical model was developed in order to estimate the spread of grout considering the geometry of a plug of Bingham material and velocity during the grouting process. Numerical simulations were performed for a flow of grout in a rectangular channel network and radial disk, where flow was formulated on the basis of the grout velocity, rheological properties and pressure difference. The plug thickness of the grout was estimated iteratively, where both the grout velocity and the grout head at the end of the channel are known.

Estimation of the plug thickness of grout in a circular pipe was made by Håkansson (1993). In addition, effects of the rheological properties on the estimation of the grout spread were discussed. Analytical solutions for the estimation of the grout spread in a disk around the borehole were presented by Gustafson and Claesson (2005). It was assumed that the flow can take place only in a part of the fluid for a Bingham material, which implies that a stiff plug is formed in the center of the flow channel, surrounded by a plastic flow zone. The maximum spread of grout can be determined by using the force balance between the grouting pressure and resisting water pressure, ΔP , as shown in equation 13. The relative spread of grout was defined as shown in equation 15.

The relative spread of grout was defined on the basis of the relative time (t_D), which is the ratio between the grouting time and characteristic time and can be shown as

$$t_0 = \frac{6\mu_g \Delta P}{(\tau_0)^2} \tag{20}$$

The relative time, t_D, as a function of $I_{D,P}$ for a circular pipe can be derived as (Gustafson et al. 2013)

$$t_D = \frac{I_{D,P}}{6(1-I_{D,P})} + \frac{1}{36}\ln\left[\frac{3(1-I_{D,P})^2}{3+2I_{D,P}+I_{D,P}^2}\right] - \frac{5\sqrt{2}}{36}\arctan\left(\frac{I_{D,P}\sqrt{2}}{I_{D,P}+3}\right) \quad (21)$$

and a function of $I_{D,C}$, for a rectangular channel can be derived as

$$t_D = \frac{I_{D,C}}{3(1-I_{D,C})} + \frac{2}{9}\ln\left[\frac{2(1-I_{D,C})}{2+I_{D,C}}\right] \quad (22)$$

The analytical solution for equations 21 and 22 cannot be solved explicitly for I_D as a function of t_D. Therefore, approximate solutions were derived by Gustafson and Stille (2005) and can be shown as

$$I_D \approx \sqrt{\frac{t_D^2}{4(\delta+t_D)} + \frac{2t_D}{\delta+t_D}} - \frac{t_D}{2(\delta+t_D)} \quad (23)$$

where, $\delta = 0.6$ for one dimensional channel and $\delta = 3$ for a radial flow.

For a two dimensional radial disk, similar approximate analytical solutions were proposed by El Tani (2012). The difference between the approximate solutions from Gustafson and Stille (2005) and El Tani (2012) is the assumption regarding the change of the plug thickness. Based on the hypothesis that a radial flow is always deforming and that there could only be a plug if the flow is stopped, El Tani (2012) derived the equation for radial flow assuming a constant plug thickness along the radial disk (Lipscomb and Denn 1984). In contrast, Gustafson and Stille (2005) and Hässler (1991) used the equation of radial flow provided by Bird et al. (1983) and considered a change of plug thickness along the radial disk.

2.5.3 Bingham number (B_N)

To simplify the determination of the velocity and plug thickness of the grout front for one dimensional and two dimensional flows, a dimensionless parameter, the Bingham Number (B_N), was used. B_N was introduced by Bird et al. (1983). This was further shown as a dimensionless yield stress that was the governing factor for extrusion flows, and entry and exit flows of Bingham materials (Papanastasiou 1987; Abdali et al. 1992). It was shown that, with an increased B_N, the rigid core or the stiff plug of the Bingham material is increased. The Saint-Venant number (*Sen*), derived from the Reynolds number (Re) and Hedström number (He), which is actually the same as B_N, was used to show the change of the plug thickness inside a circular tube and flat channel. With an increased *Sen* number, an increase of the solid core and the relative annular gap was calculated (Bukhman et al. 1982). The *Sen* number was also used to estimate the relative plug thickness inside a circular pipe (Håkansson 1993). However, in this work, the dimensionless parameter is defined as the B_N and can de expressed as

$$B_N = \frac{b\tau_0}{\mu_B \overline{v_z}} \tag{24}$$

where, b is the thickness of the rectangular channel, the radial disk or the diameter of the circular pipe and $\overline{v_Z}$ is the mean velocity of the grout front. As shown in equation 24, the B_N is the governing factor for determining the mean velocity, $\overline{v_Z}$. For a two dimensional flow, $\overline{v_Z}$ is a function of the radial distance; therefore, B_N will change accordingly.

2.5.4 Plug thickness and shear rate

A plug region is formed inside a Bingham fluid where the shear stress is below the yield stress. The relative plug thickness can be determined from the expression of velocity for a one dimensional or a two dimensional geometry. The mean velocity for a Bingham fluid in a pipe can be obtained from the volumetric flow rate, by inserting the Bingham model into the expression for flow rate, which is known as the Buckingham – Reiner equation and can be shown as

$$\overline{v}_x^B = \frac{\tau_0 R}{4\mu_B} \frac{\left(1 - \frac{4}{3}\xi_{pipe} + \frac{1}{3}\xi_{pipe}^4\right)}{\xi_{pipe}} \tag{25}$$

To determine the relative plug thickness, equation 25 can be rearranged and shown as

$$\xi_{pipe}^4 - 4\left(\frac{6}{B_N} + 1\right)\xi_{pipe} + 3 = 0 \tag{26}$$

The solution for equation 25, as solved by Håkansson (1993) can be shown as

$$\xi_{pipe} = \frac{1}{2}\left[-\sqrt{4\sqrt{\frac{1}{4}(\alpha+\beta)^2 - 3} - (\alpha+\beta)} + \sqrt{\alpha+\beta}\right] \tag{27}$$

where

$$\alpha = \left[\sqrt{64\left(\frac{6}{B_N}+1\right)^4 + 64} + 16\left(\frac{6}{B_N}+1\right)^2\right]^{\frac{1}{3}} \text{ and}$$

$$\beta = \left[-\sqrt{64\left(\frac{6}{B_N}+1\right)^4 + 64} + 16\left(\frac{6}{B_N}+1\right)^2\right]^{\frac{1}{3}}$$

The expression for flow in a channel for a Bingham fluid can be shown as

$$v_{channel} = \frac{\tau_0 b}{12\mu_B} \frac{\left(1 - 3\xi_{channel} + 4\xi_{channel}^3\right)}{\xi_{channel}} \tag{28}$$

To determine the relative plug thickness in a rectangular channel, equation 28 can be rewritten in the following way

$$\xi_{channel}^{3} - 3\left(\frac{1}{B_N} + \frac{1}{4}\right)\xi_{channel} + \frac{1}{4} = 0 \tag{29}$$

The closed form solution for the relative plug thickness for the flow of Bingham material inside a rectangular channel can be shown as (Hässler 1991)

$$\xi_{channel} = 2\sqrt{\frac{1}{B_{N,channel}} + \frac{1}{4}}\cos\left(\frac{\pi}{3} + \frac{1}{3}\arccos\left(\frac{1}{8\left(\frac{1}{B_{N,channel}} + \frac{1}{4}\right)^{1.5}}\right)\right) \tag{30}$$

The flow of Bingham material in a radial disk is a two dimensional flow. The difference from the radial flow from a channel is that there is also a spread in the transverse direction. The flow, Q, can be shown as

$$Q = 2\pi r b v_{radial} \tag{31}$$

Q remains constant for a radial flow, although, the pressure gradient is nonlinear and changes as a function of r. The expression for velocity can be developed in the same way as for one dimensional flow, as shown in equation 28. However, ξ_{radial} must be used. The ξ_{radial} can be obtained using the expression similar to that in one dimensional flow in equation 30; however v_{radial} should be used for the determination of B_N. Due to a nonlinear distribution of pressure difference, the velocity of the grout front would be different for other parts at a certain section. The estimated B_N for two dimensional flow in this work should therefore be regarded as the B_N at the grout front.

The wall shear rate can be calculated from the Bingham model definition. The distribution of shear stress at any cross section is always linear and independent of rheological models. The Bingham equation can be re arranged and the shear rate can be shown as

$$\dot{\gamma}_W = \frac{\tau_0}{\mu_b}\left(\frac{1}{\xi} - 1\right) \tag{32}$$

3 Materials and Methodology

3.1 Materials

Owing to their ease of preparation and use, wide availability and relative low cost, cement based materials are the most commonly used grouts for permeation grouting. In this work, Cementa IC30, a relatively fine cement with a water/cement ratio of 0.6 – 1.0 (by weight), was used because of its frequent applications in practice. IC30 is a sulphate resistant, chromate reduced and low alkali grouting cement. The largest particle size is 30 microns. Cementa SetControl II was used as an additive. According to the manufacturer, this is a high performance binding time regulator that is suitable for grouts based on Cement.

The mixing was performed using a high speed dissolver DISPERMAN CV 3-PLUS (VMA GETZMANN GMBH). An impeller geometry was used and a rotational speed of 2500 rpm was applied during mixing. The grout was mixed for 4 minutes.

A commercial hair gel (Gatsby Water Gloss/ Wet Look Soft) was used as a model fluid following earlier work (Moller et al. 2009 b).

3.2 Experimental flow loop

Two different types of experimental set-ups were used for the field like and laboratory based conditions. The standard grouting rig, UNIGROUT E22H from Atlas Copco, was used to keep conditions the same as in the field. The flow was circulated through a flow loop consisting of the grouting rig UNIGROUT E22H, UVP+PD test section and a LOGAC™ flow/pressure meter. LOGAC™ was used as a reference for the flow rate determined by UVP. The schematic illustration of the experimental set-up used for the field like conditions is shown in Figure 9.

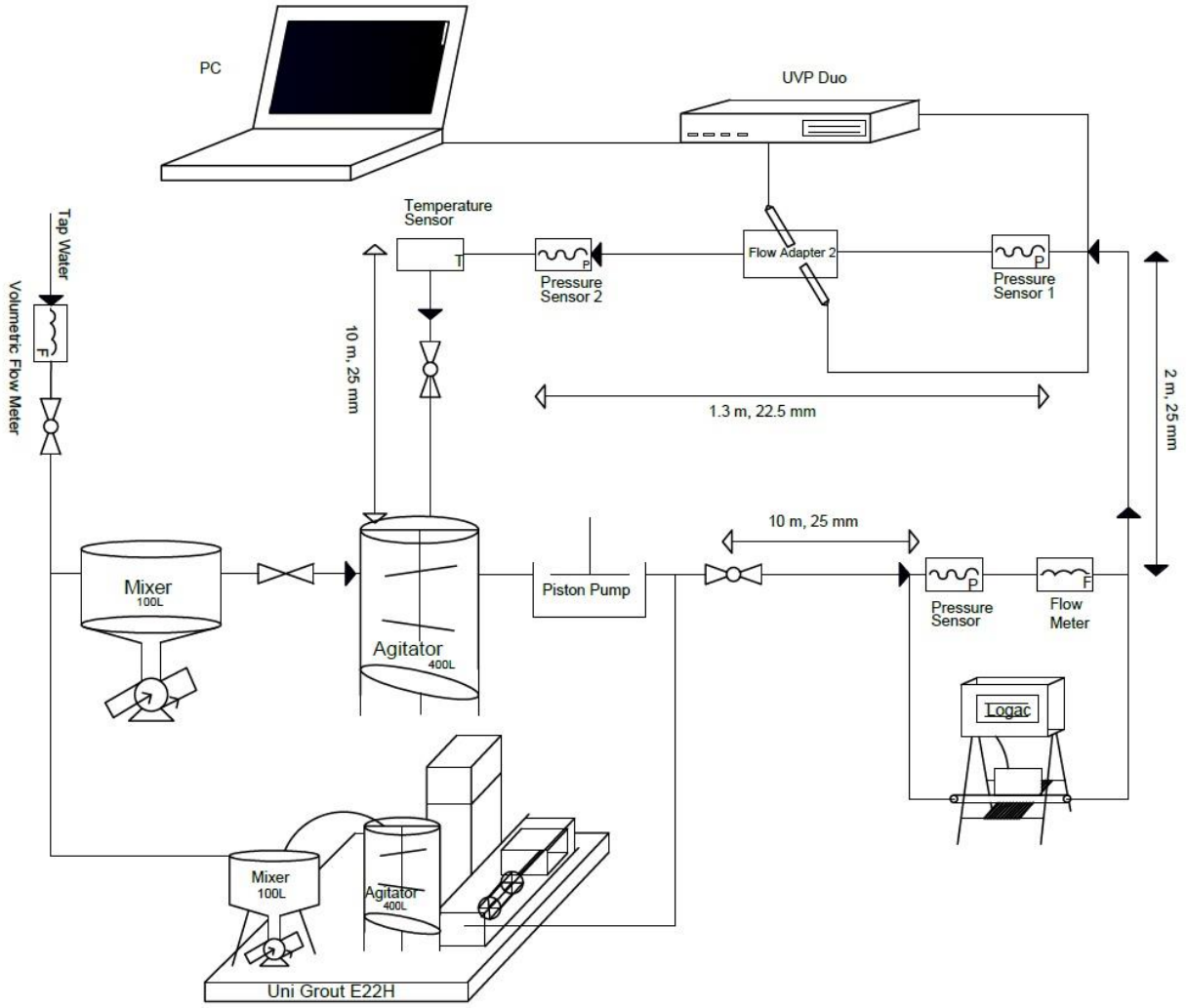

Figure 9 Experimental set-up used for the field like conditions

A laboratory based flow loop was designed consisting of a helical rotor progressive cavity type pump in order to achieve a stable flowing condition during the determination of the rheological properties. The flow was circulated through a flow loop consisting of a storage tank, a progressive cavity single screw pump, the UVP+PD test section, the LOGAC™ flow meter and temperature sensors. The objective was to obtain a steady flow using a progressive cavity pump and a simpler set-up by excluding the UNIGROUT E22H. A schematic illustration of the experimental set-up is shown in Figure 10.

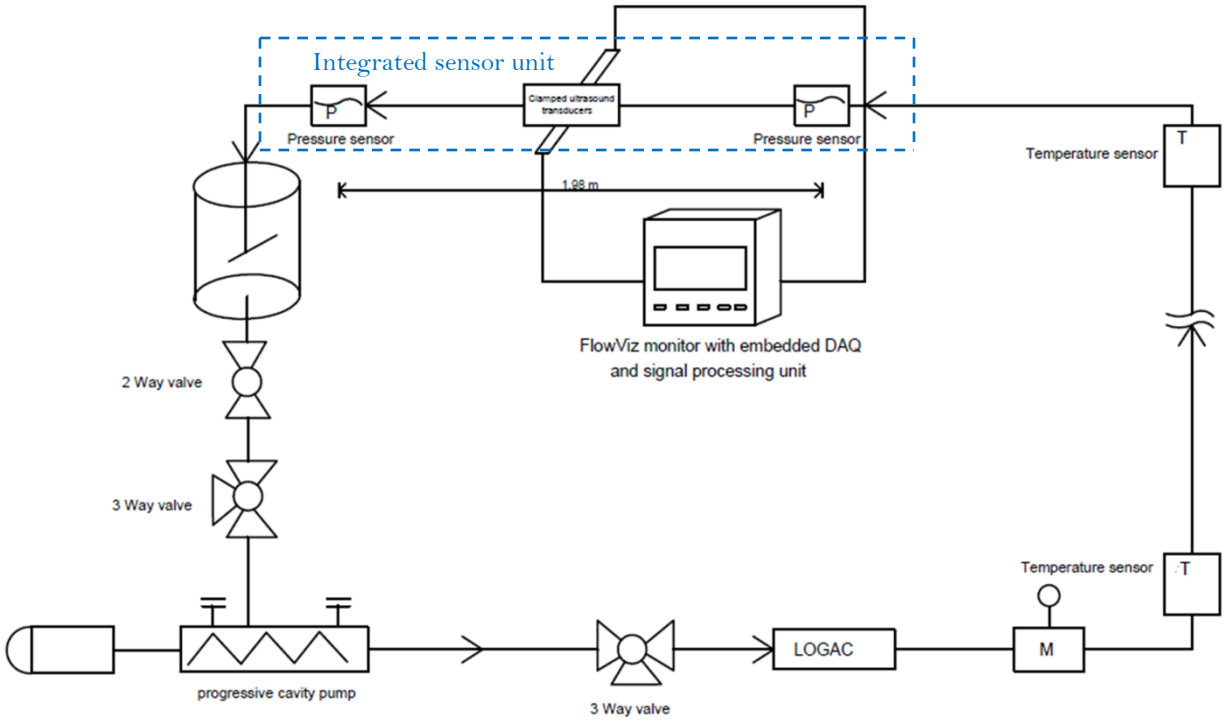

Figure 10 Experimental set-up used for the laboratory based conditions

3.3 UVP+PD instrumentation

3.3.1 Ultrasound transducers and flow cell

Two different types of ultrasound transducers were used in this project. Cement grout is an attenuating material, and standard commercial transducers are not capable of emitting sufficient acoustic energy to measure the velocity profile at least across the pipe radius (pipe wall to center). For this reason, custom made delay line ultrasound transducers were used. A delay line is a material fixed ahead of the transducers that reduces the near field distance. As a result, velocity profiles just in front of the transducer face can be measured. A flow adapter cell was developed and fitted with one pair of custom made delay line 4 MHz transducers. The inner diameter of the flow adapter was 22.5 mm. The flow adapter material was stainless steel. Transducers were mounted in flush with the pipe through the cavities with a diameter equal to the housing diameter of the transducers. The delay line material contained the near-field distance, and the focal point was designed at the pipe wall and delay line surface interface.

The flow adapter and transducer installation used for this experiment are shown in Figure 11.

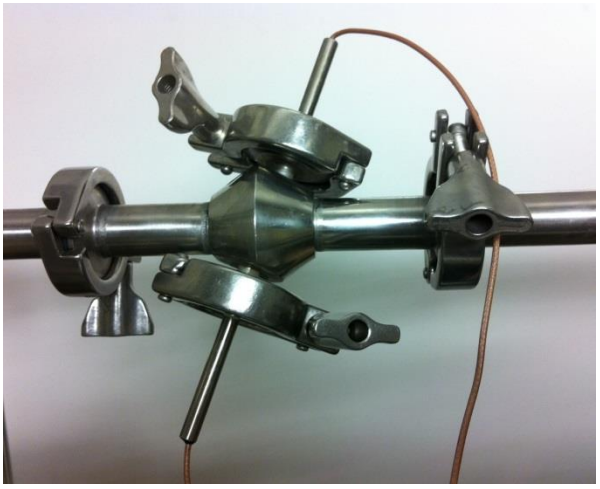

Figure 11 Flow adapter cell consisting of delay line ultrasound transducers

For the experiments carried out in field like conditions, two 4 MHz ultrasound transducers (TR0405LH-X, Signal-Processing SA, Savigny, Switzerland), were fitted with the flow adapter. These transducers allow measurements directly from the transducer front, implying that more or less zero velocity at the wall can be recorded. The active and outer diameters of the transducers are 5 mm and 8 mm, respectively. The transducers were fixed inside the flow adapter in the horizontal plane to minimize the sedimentation effect and were placed opposite to each other with a Doppler angle.

Delay line transducers might often lack the emitted acoustic energy and robustness (Rahman et al. 2012). Delay line absorb acoustic energy and remain in contact with the tested fluid. As a consequence, a robust, non-invasive ultrasound sensor unit, capable of emitting sufficient acoustic energy, mounted outside of the stainless steel pipe, was required. For the experiments in laboratory based conditions, a novel non-invasive sensor unit was developed by SP and their partners that consist of ultrasound transducers, wedges, absorber, and acoustic couplants. This was the first time experiments were performed to measure a profile non-invasively through high grade stainless steel. The non-invasive sensor unit with the mounting device is shown in Figure 12.

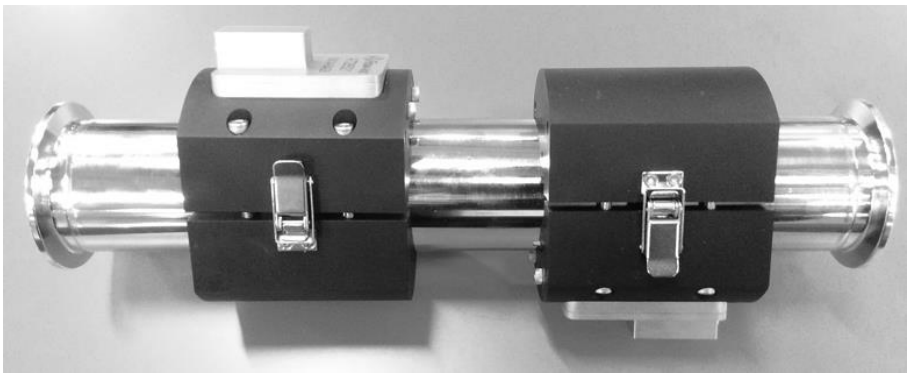

Figure 12 Non-invasive sensor with mounting device

3.3.2 Instrumentation

Two types of pulser-receiver hardware were used in this work. The measurements performed in the field like conditions were made with a UVP-DUO MX (Met-Flow, SA, Lusanne, Switzerland) model with a multiplexer. The instrument firmware and driver software were modified to allow access to the demodulated echo amplitude data (DMEA; raw data that cannot be obtained using standard instruments). The UVP Duo instrument and other hardware devices were connected to a master PC via Ethernet, and a DAQ card (National Instruments, ABB). MatLab based software with a graphical user interface (Rheoflow) was used to control all hardware devices for data acquisition, signal processing, visualization of the data and real time monitoring of the rheological properties. UVP data acquisition was implemented using an active X library (Met-Flow, SA). A high speed digitizer card (Agilent Acquiris) was used as an integral part of the data acquisition scheme, enabling simultaneous measurements of the velocity profiles and acoustic properties. Two differential pressure sensors (ABB 256DS, ETP80,ABB Automation Technology Products AB, Sollentuna, Sweden), 45V DC, 20 mA, PS 40 bar, were used to measure the pressure difference over a distance of 1.3 m for 4 MHz transducers.

3.3.3 Flow-Viz industrial rheometer

The limitation associated with the UVP-DUO MX hardware is that the spatial resolution is fairly low. In addition, the data acquisition (DAQ) and signal processing platform are not fully integrated, therefore, lacks in robustness. For that reason, an industrial rheometer, 'Flow-Viz', capable of emitting ultrasound pulses with a high sampling rate, developed at 'SIK- The Swedish Institute for food and Biotechnology' was used for further investigation of the rheological properties. The Flow-Viz rheometer is a complete integrated and fully digital platform for pulsed ultrasound measurements with an embedded DAQ and onboard signal processing capabilities.

Figure 13 Flow-Viz industrial rheometer

The system consists of pulser receiver hardware and a pair of custom made, non-invasive sensor units, clamped on to a pipe section and capable of emitting sufficient acoustic energy to perform non-invasive measurements of the velocity profiles through the stainless steel pipe. The non-invasive sensor unit consists of several components, such as a high power ultrasound transducer, wedge, attenuator and different couplant materials. The configuration provides optimum acoustic beam properties, such as beam forming, focusing and coupling, and impedance matching (Wiklund et al. 2012). An image of the 'Flow-Viz' industrial rheometer is shown in Figure 13. The Flow-Viz technology has a spatial resolution of 11 um due to its high sampling capabilities; this means that over 1000 local velocity measurements across the pipe radius (11 mm) can be obtained. Detailed information concerning the velocity profiles, i.e., slip at the pipe wall, change of the shape of the velocity profile due to rheology can thus be visualized. The Flow-Viz system is a fully integrated hardware platform comprising a total of four analog and digital electronics boards. The electronics enable simultaneous UVP, pressure and temperature acquisition and signal- processing from multiple sensors. It also provides real - time communication capabilities to an industrial PC (Ricci et al. 2006; Ricci et al. 2012).

3.4 Conventional off-line rheometry

3.4.1 Equipment

A TA instrument AR 2000 EX rheometer was used to perform the rheological measurements of cement grout. The AR 2000 EX rheometer can be operated at stress controlled, rate controlled and strain controlled mode. The concentric cylinder and vane geometries were used to perform the different tests.

A standard DIN concentric cylinder geometry was used to perform stress ramp tests. The stator inner and rotor outer radius was 15 mm and 14.65 mm, respectively. The immersed

height was 42.25 mm and the gap was 5912 mm. The cylinder surface was roughened with fine sand to eliminate the slip at the cylinder wall.

Standard vane rotor geometry was used as a wide gap vane to perform the stress ramp tests, constant rate tests and creep tests. The stator inner and rotor outer radius were 15 mm and 7 mm, respectively. The immersed height was 38 mm and the gap was 4000 mm.

A Brookfield DV-II Pro viscometer was used to perform the stress relaxation test. This viscometer can be operated at shear rate controlled mode. The maximum applicable speed is 200 rpm, and the measurable viscosity range is 0.015 Pa – 6000 Pas. Two types of concentric cylinder (spindle), SC4-31 and SC4-34 were used for the tests.

3.4.2 Experimental technique

Vane test performed at constant shear rate

The vane method offers the superiority of eliminating the slip at cylinder wall interface and minimum disturbance when the vane is immersed in the sample (Nguyen and Boger 1983). The vane method was used to determine the static yield stress of cement grout. The vane was immersed in to the grout sample and rotated at a constant shear rate (CSR) of 0.01 s-1 for 30 seconds. The corresponding torque was measured and the shear stress was calculated. It is therefore, considered to be the direct measurement of static yield stress. A resting period of 5 minutes followed after the rotation. The resting period was provided for the structural buildup of the suspension. The change of the static yield stress with time was measured for 50 minutes.

Stress ramp test

Stress ramp tests were performed under a controlled stress environment (CSS) in order to determine the yield stress of cement grout. A wide gap, vane geometry was used to perform the stress ramp tests. A ramp of 0.2 Pa/s was applied, and the stress was increased from 0.001 - 15 Pa. This was followed by a down ramp where the applied stress was decreased from 15 - 0.001 Pa. The corresponding torque was measured, and the shear rate and the viscosity were calculated. A resting period of 5 minutes was provided after each up-down ramp. The up-ramp provided the static yield stress, which is required to break the particle bonding and initiate the flow. In contrast, prior to the down-ramp, the grout sample was sheared at a broken down state. Therefore, the dynamic yield stress was determined during the down

-ramp. The up-down ramps were performed for 50 minutes, therefore allowing measurements of the change of the static and dynamic yield stress.

Creep test

Creep tests were done to define the viscosity bifurcation of cement grout. A wide gap, vane geometry was used for the tests. At a controlled stress environment, six different stresses, 0.2, 1. 3, 5, 6.5 and 8 Pa, were applied for different sample grouts for 20 minutes. The corresponding torque was measured and the shear rate and, viscosity were determined. Due to viscosity bifurcation, unlike the case of yield stress fluids, the cement grout stops flowing below a critical shear stress and starts flowing when a higher stress is applied. In addition, the viscosity increases with time when the applied stress is below the critical yield stress and decreases when the applied stress is higher. This phenomenon has been shown earlier for other yield stress fluids (Coussot et al. 2002b).

Stress relaxation test

Stress relaxation tests were done to determine the dynamic yield stress of cement grout. In these tests, the spindle was rotated at a constant speed and suddenly stopped to a rotational speed of zero rpm. If the sample is a true yield stress fluid, it should possess a residual stress that will remain at a relaxed state for a considerably longer period of time. It is therefore, considered to be the dynamic yield stress (Nguyen and Boger 1983; Håkansson 1993). The grout sample was rotated at a constant speed for 60 seconds, which was followed by a sudden stop. The corresponding torque was measured and the shear stress was determined. In this work, three arbitrarily rotational speeds, i.e., 10, 100 and 200 rpm, were used. Each rotation of 60 seconds was followed by a resting period of 5 minutes, allowing measurement of the change of the dynamic yield stress was measured.

4 Results and discussion

4.1 In-line measurement of the rheological properties of cement grout (Paper I)

4.1.1 In-line measurement of the velocity profiles

The feasibility of using the UVP+PD method to determine the rheological properties of cement grouts depends on the measurement of the velocity profiles. Since it was possible to measure the velocity profiles for w/c ratios down to 0.6, at least up to the center of the pipe, the UVP+PD method was found capable of determining the rheological properties directly in-line under field like conditions. The visualization and shape of the velocity profiles of cement grouts was an important finding, since it is not possible to achieve using any other method and was performed for the first time for cement based grouts. Velocity profiles measured for a water cement ratio of 0.8 is shown in Figure 14. A piston type of pump was used for pumping the grout and wide fluctuations of the velocity profiles due to a change in the pressure were observed. As shown in the Figure 14, the maximum velocity changed from 0.1 m/s – 0.8 m/s, which cannot be observed using any other commercial flow meters. In addition, a negative velocity was seen, which was due to the backstroke of the piston. Nevertheless, for the w/c ratio of 0.6, the velocity profiles were distorted at the center of the pipe due to the strong attenuation of the ultrasound energy. Moreover, the transducers were installed in cavities into a flow adapter, and clogged cement particles were observed that decreased the penetration length due to the strong attenuation. As a result, a non-invasive, clamp-on type device capable of emitting higher acoustic energy was required.

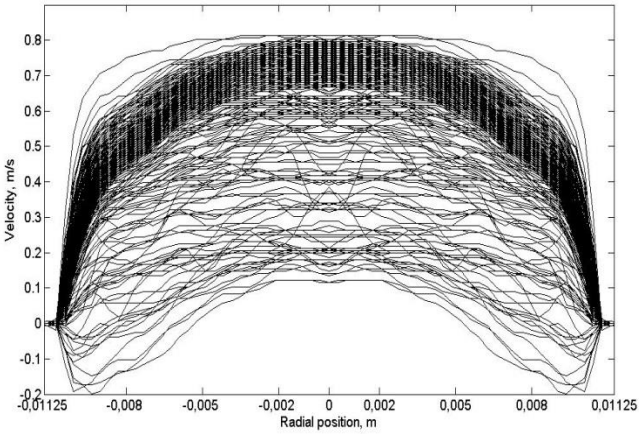

Figure 14 Velocity profiles for w/c ratio 0.8, sampled over 3 minutes

4.1.2 Comparison of rheological properties

Rheological properties were determined using the Herschel Bulkley model fitting procedure. This model was chosen since it includes a yield stress and exhibits a shear thinning behavior, which resembles the behavior observed in cement grouts. As expected, a trend of increased yield stress was observed for a thicker suspension, i.e. w/c ratio of 0.6. A change in the rheological properties, i.e. increased yield stress and viscosity with time, was observed for w/c ratios of 0.6 and 0.8.

The rheological properties obtained off-line using the rotational rheometer and the corresponding shear stress versus shear rate curve is shown in Figure 15. As expected the grouts all show a shear thinning behavior with increasing shear rate. It was observed that the yield stress increases with a decreasing water/cement ratio within the first hour after mixing, as expected. However, a higher yield stress was also observed for w/c ratio 0.8 since the sample was measured after a longer period of time after mixing. A time dependent behavior was observed by the yield stress increasing with time for both w/c ratios 0.6 and 0.8, which agrees well with the in-line results. The largest discrepancy in the flow curves is associated with the sample measured 66 minutes after the mixing for w/c ratio 0.6. It is believed that this is an erroneous result caused by a non-representative sample taken from the field equipment and into the laboratory, as discussed above. It should be noted that the problem of obtaining a representative sample from the process clearly illustrates the main disadvantage of conventional off-line measurements for process monitoring and control and thus gives a strong motivation for measuring in-line, directly in the process pipe, using e.g. the UVP+PD method.

The rheological properties obtained in-line using the UVP+PD method and the corresponding shear stress versus shear rate curve is shown in Figure 16. From the shear stress vs. shear rate plot shown in Figure 16, it was observed that the yield stress increases with a decreasing water/cement ratio and with increasing time after mixing, which was expected. The yield stress for water cement ratio 0.6 showed only a marginal increase when comparing the measurements taken after 67 minutes and after 89 minutes respectively. This can however be explained by the short difference in time after mixing. For water cement ratio 0.6 it was difficult to obtain a stable flow condition without increasing the total pressure in the system above the maximum allowed pressure level for the testing equipment. A commercial additive SetControl II was therefore added as it gradually increases the viscosity with time. The effect was more pronounced for water cement ratio 0.8 than for water cement ratio 0.6, but this is partly explained by the longer times from mixing to measurement. It was not possible to continue the measurements after 89 minutes for water cement ratio 0.6 due to experimental problems with the grouting rig but also because the effects of SetControl II as a function of time from mixing had not been investigated under the experimental conditions prior to the in-line experiments (i.e. from higher to lower shear rate).

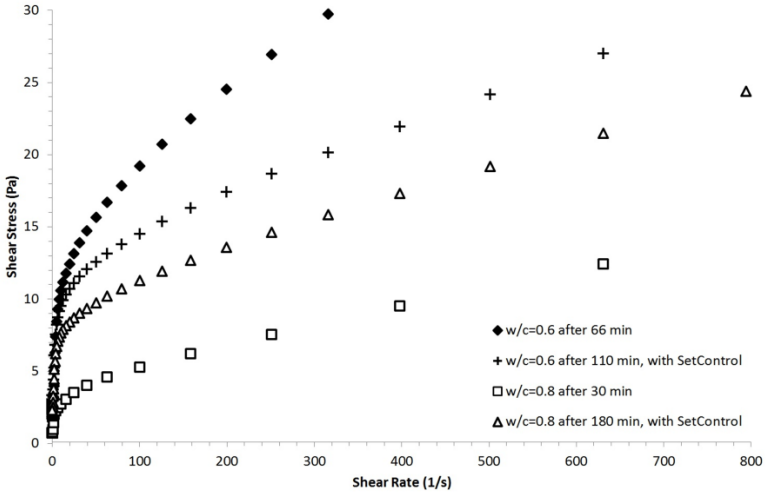

Figure 15 Flow curves of different w/c ratios measure using the off-line rheometer

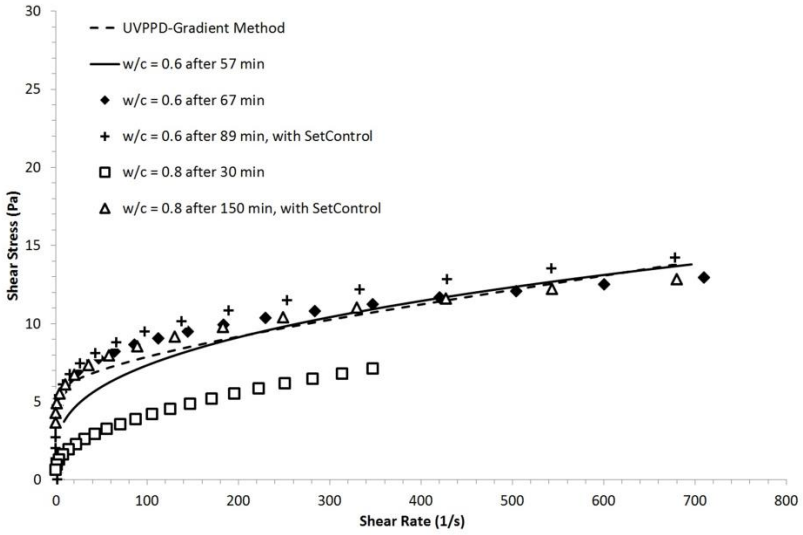

Figure 16 Measurement of flow curve using the UVP+PD method

4.2 Change in the rheological properties of cement grout with concentration and time (Paper II)

Since the yield stress and viscosity of cement grout change with concentration and time, a further study was done to determine the change in the rheological properties directly in-line. A novel non-invasive sensor unit, capable of emitting sufficient acoustic energy, was tested. Velocity profiles were measured for w/c ratios of 0.6-1.0. It was possible to measure velocity profiles for w/c ratios down to 0.6, as shown in Figure 17. It can be seen in Figure 17 that the velocity profiles were measured until the center of the pipe, and a plug flow can be seen at the center of the pipe. As a result, the change in the rheology of cement grout due to concentration and time can be visualized directly in-line. It is evident from the shape of the velocity profile that, at higher w/c ratio, e.g. w/c 1.0, the shape of the measured velocity profile indicated that it was fairly Newtonian, in contrast to a lower w/c ratio, where a Bingham behavior, i.e. a plug flow, is visible. In addition, the velocity profile was measured beyond the center of the pipe, which indicates the improvement in the non-invasive sensor unit in terms of emitting sufficient acoustic energy.

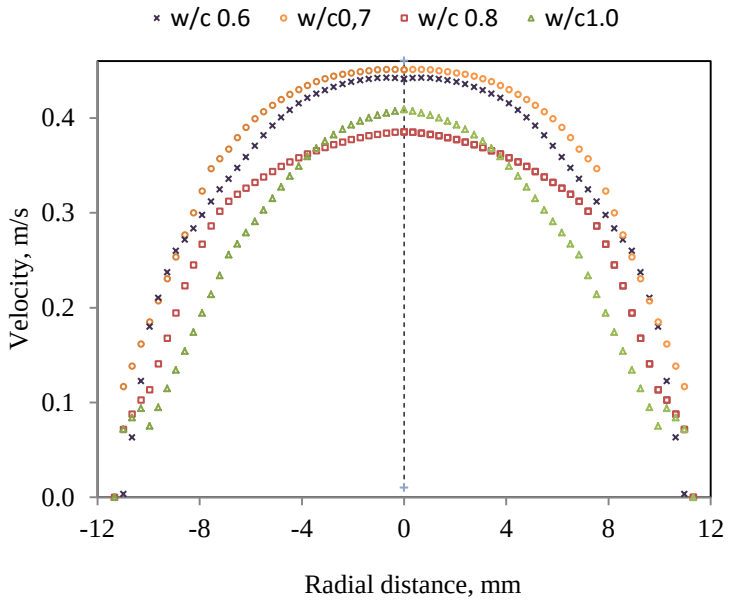

Figure 17 Velocity profiles for w/c ratios of 0.6, 0.7, 0.8 and 1.0 measured by the non-invasive sensor unit

The rheological properties were determined using the Bingham, Herschel-Bulkley (H-B) models and a non-model approach, known as 'gradient method'. As expected, an increased yield stress was observed for a higher concentration and with time. In addition to using the rheological models, yield stress and viscosity were determined with non-model approaches, e.g. the gradient method and tube viscometry concept, and are compared. With the gradient method, since no model fitting was used, it is the actual measured rheological behavior that is presented. An increase in the yield stress and viscosity of cement grout was observed. A very high yield stress was observed for the w/c ratio of 0.6. This is expected, however, due to the thicker concentration. Off-line measurements were made with conventional rotational rheometers, and good agreement was found with the in-line results.

4.2.1 Change of the yield stress determined by Bingham model

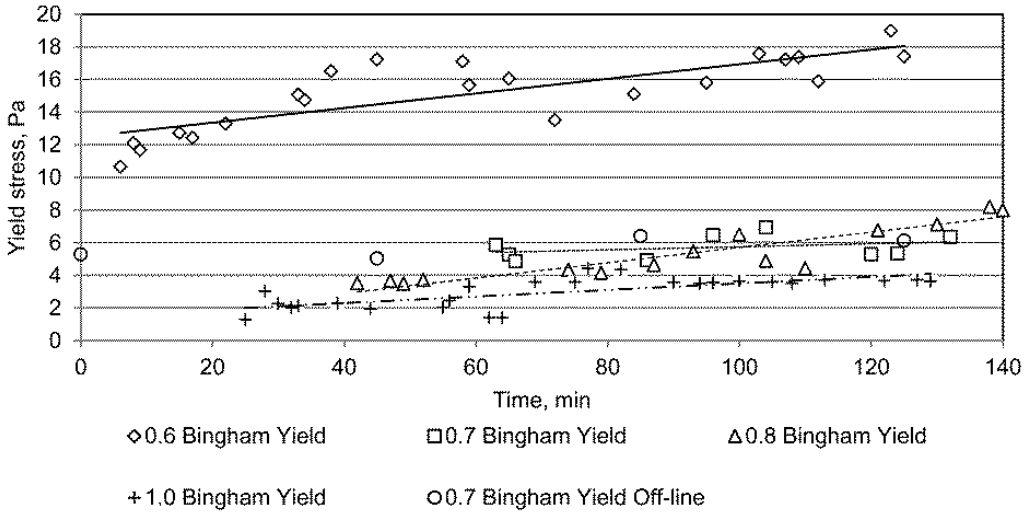

Figure 18 Change of yield stress determined using the Bingham model

The yield stresses determined by the Bingham model are shown in Figure 18. The increases in the yield stress and viscosity due to hydration with time and for different concentrations are visible. The highest value of yield stress was observed for the w/c ratio of 0.6, which was expected owing to the highest concentration of cement particles. It must be noted that the earliest measurement was made 25 minutes after the mixing of the cement. For easier illustration, the increase in the yield stress and viscosity is shown by linear trend lines. The trend of increased yield stress with time was observed for w/c 0.6. However, some discrepancies, e.g. decreased yield stress, can be seen for the time period from 60-80 minutes, which can be explained by the shape of the velocity profile. Since the measured velocity profile was fitted using a mathematical model, a slight distortion in the measured data will yield a different gradient at the velocity profile and will therefore result in an inaccurate rheological property value. An expected trend of the increased yield stress was observed for w/c ratios of 0.7, 0.8 and 1.0. The yield stress determined for the w/c ratio of 0.7 is in good agreement for both the in-line and off-line measurements. The progress of yield stress with time was mildest for w/c ratio 1.0, which was due to the thinner suspension of cement.

4.2.2 Change of the yield stress determined by Herschel-Bulkley (H-B) model

The H-B model was chosen to simulate the rheological behavior of cement grout since it consists of a yield stress and exhibits a shear thinning behavior consistent with many dense suspensions. As can be seen from the shear stress vs. shear rate curve, fitted by the H-B model in Figure 19, a higher shear stress was observed for a higher concentration of cement

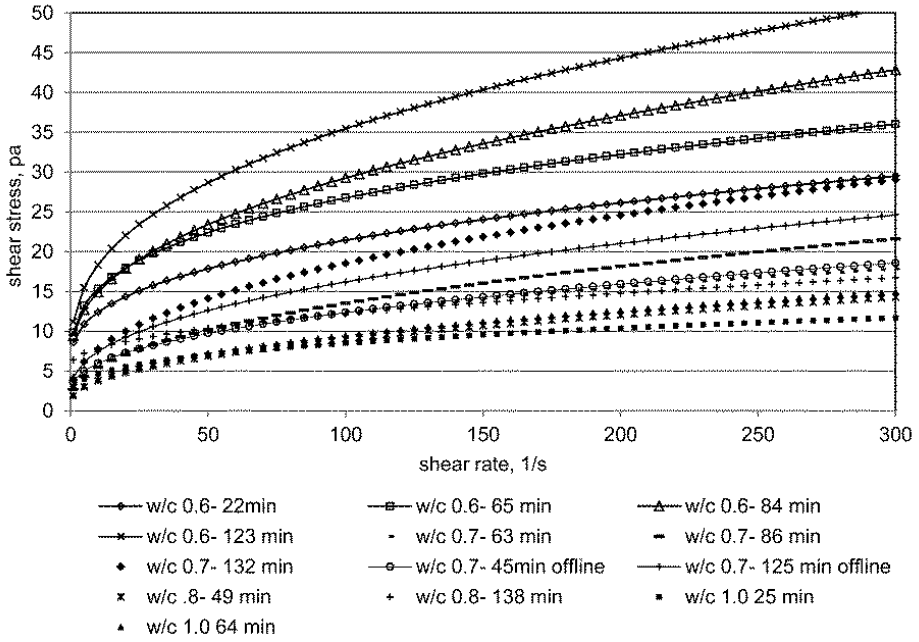

Figure 19 Change of yield stress determined using the Herschel-Bulkley model

grout. Time dependent behavior was also observed, since a higher shear stress was observed after a longer period of time, owing to hydration of the cement grout. A comparatively higher yield stress and shear stress were observed for w/c ratio of 0.6, in comparison with w/c ratios 0.7, 0.8 and 1.0, which indicates a shorter setting time resulting from a thicker concentration. A similar shear stress for the w/c ratio 0.8 after 138 minutes was observed as compared to w/c 0.7 after 63 minutes, which was due to the longer time after mixing for the w/c ratio of 0.8. Off-line measurements were made for w/c ratio 0.7, and very good agreement was found between the in-line and off-line measurements. Since viscosity is obtained from the gradient of the shear stress curve vs. shear rate curve, Figure 19 can illustrate that the difference in viscosity was more pronounced for different w/c ratios at a lower shear rate.

4.2.3 Change of the yield stress determined by Gradient method

The gradient method is a non-model approach that is capable of performing direct measurements of rheological properties instead of using any rheological fitting procedure. Figure 20 shows time dependent behavior, i.e. increasing shear stress with time, for w/c ratios 0.7 and 1.0. As expected, a higher shear stress was exhibited by w/c ratio 0.7 in comparison with w/c ratio 1.0 because of a thicker suspension. The distorted shapes at the higher shear rate region of the shear stress vs. the shear rate curve are due to the distortion

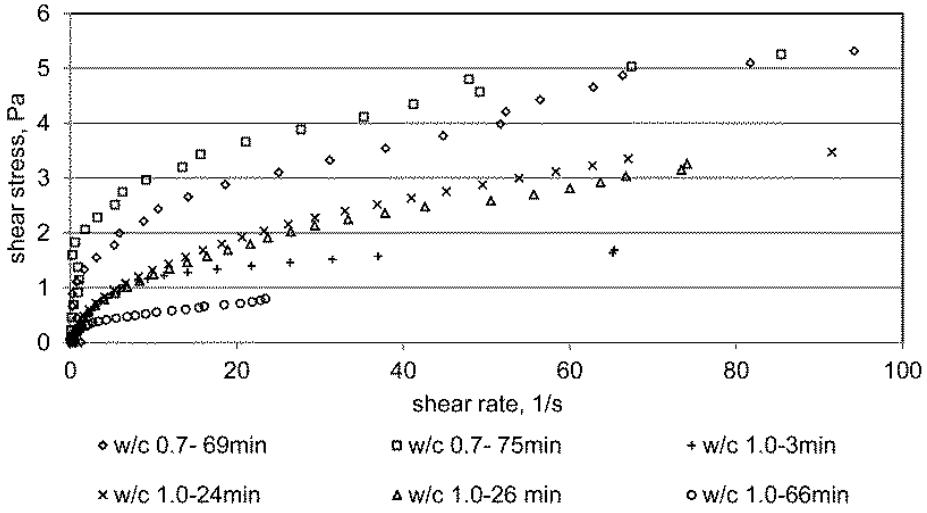

Figure 20 Change of yield stress determined using the non model approach

in the shear rate distribution. Detection of the correct wall position and an accurate velocity profile measurement in the near wall region can eliminate distortion at the higher shear rate region. For the w/c ratio 1.0 after 66 minutes, a lower shear stress was observed as compared with w/c ratio 1.0 after 24 and 26 minutes.

It must be noted that the flow rate was not the same for both samples. As can be seen, a lower flow rate, i.e. a lower shearing rate, yielded a lower shear stress, which indicates a different structural breakdown and recovery of the material at different velocities, i.e. flow rates.

4.2.4 Determination of the volumetric flow rate

The volumetric flow rate was determined by integration of the velocity profiles and this was subsequently compared with the results obtained with the LOGAC™ and the commercial electromagnetic flow meter. As shown in Figure 21, for the field grouting rig UNIGROUT E22H, a fluctuation of the flow rate was observed in the UVP; in contrast, the LOGAC™ yielded results over a fixed order of magnitude. This indicates that the data acquisition rate in UVP is much faster because of the higher pulse repetition frequency and provides detailed flow behavior of the cement grout in real time. Moreover, UVP is capable of providing an accurate measurement of the flow rate when it is as low as 1 liter/min, which is never possible using the commercial electromagnetic and coriolis flow meters. For the laboratory based set-up, the progressive cavity pump provided a very stable flow rate. As a result, a similar flow rate was obtained using the UVP, LOGAC™ and the commercial electromagnetic flow meter.

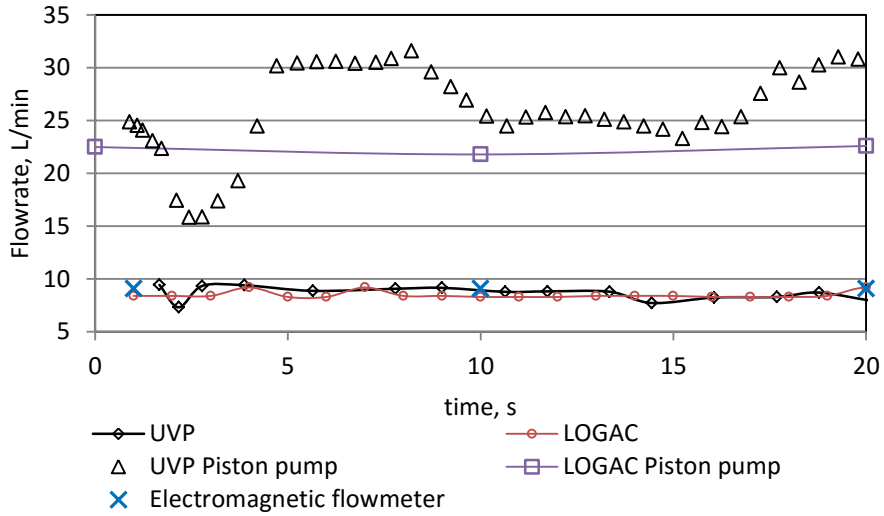

Figure 21 Volumetric flow rate determined by the UVP and measured by the LOGAC™ and the electromagnetic flow meter

4.3 Grout pump characteristics (Paper V)

Ultrasound velocity profiling (UVP) was found to be capable of faster data acquisition than the commercial flow meters and of measuring instantaneous velocity profiles. For UNIGROUT E22H, as shown in Figure 14, 512 profiles were measured over 50 seconds for the w/c ratio of 0.8. The velocity fluctuated from 0.1 m/s to 0.8 m/s, which occurred due to the pulsation of the piston pump. Moreover, a negative velocity was present that was the result of the backstroke of the piston. It is not possible to measure this fluctuation of the velocity profiles with the commercial flow meters. Moreover, the effect of pulsation on the penetration of cement grout inside a rock fracture is as yet unknown.

For the laboratory based setup, a progressive cavity type of pump was used and the pump was operated at a flow rate range of 5-7 l/minute. Velocity profiles were measured for both w/c ratios of 0.7 and 0.8. The velocity profile measurements are shown up to the center of the pipe. A mirror image is combined with the half of the velocity profiles. Figure 22 shows the velocity profile for w/c ratio 0.7, and 50 profiles were captured over a sampling period of 30 seconds, 46 minutes after the mixing. For laboratory based set-up, while using a progressive cavity pump, the flow was very stable and there is no noticeable fluctuation of the flow, compared to the piston pump.

Therefore, the pulsation of the flow can thus be synchronized with the grout pump, and UVP can be an efficient tool to determine the grout pumping characteristics.

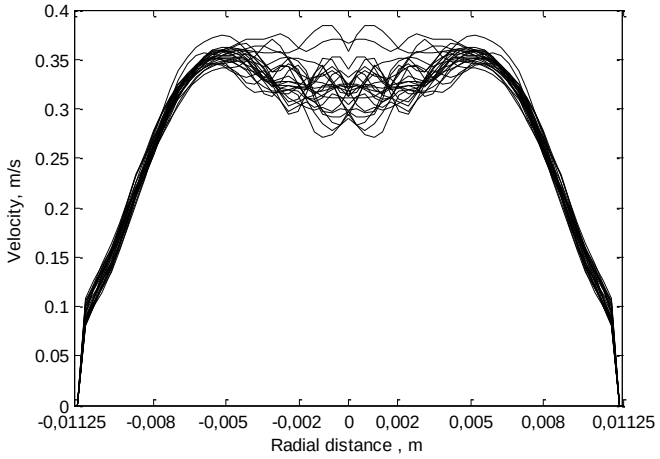

Figure 22 Measurement of velocity profiles for the progressive cavity type of pump

4.4 Measurement of yield stress of cement grout (Paper III)

4.4.1 Measurement of static yield stress

Stress ramp tests were performed to investigate the effect of hydration of cement grout for a water to cement ratio of 0.7. Prior to applying the up ramp, e.g., an applied stress of 0 -15 Pa, the sample was at rest therefore, the determined yield stress determined was the static yield stress. The results are shown in Figure 23. The interesting fact is that, even with an increased time period, the static yield stress decreased in the up curve. When cementitious materials are at rest, it is expected that the viscosity and yield stress would increase due to the buildup of the structure and flocculation during the hydration process. Calorimetric measurements were made, to further investigate the discrepancies of the change of yield stress with time. The evolution of heat with respect to time was measured for the water to cement ratio of 0.7. It was found that the heat evolution increased rapidly after mixing and reached a peak after 4-5 minutes. The peak was followed by a decrease of the heat evolution and reached a constant value after 50 minutes. It can be concluded that the dormant period started after 50 minutes. In addition, it can be concluded from the figure that the measured static yield stress was in a range of 4 -6 Pa. In contrast to simple yield stress fluids, a constant viscosity plateau was not observed at low shear stress. This can be explained by the fact that, for thixotropic suspensions, the change from a viscous state to a visco elastic solid is abrupt and that there is a range of shear rate that is not accessible when a stress controlled measurement is performed.

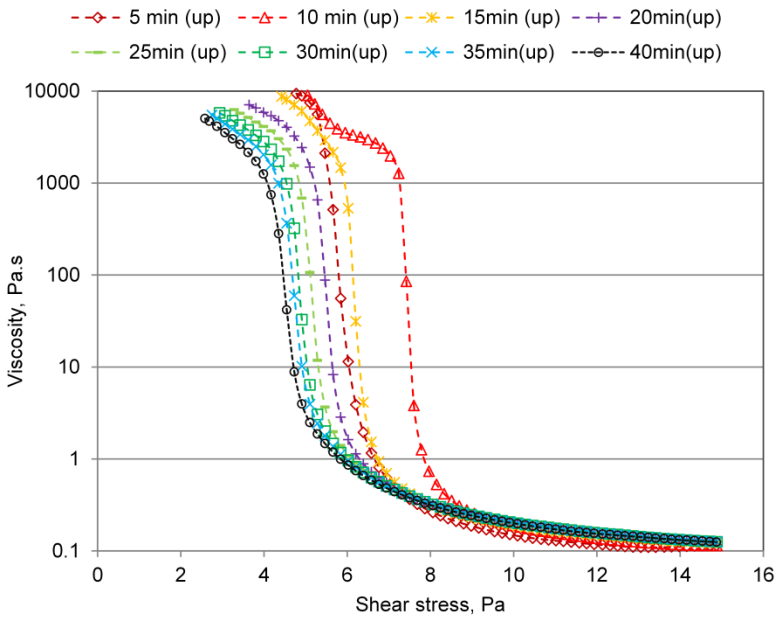

Figure 23 Stress ramp tests for w/c ratio 0.7 using vane geometry,

A direct measurement of yield stress with a vane was performed for w/c ratio 0.7 to determine the static yield stress. The results are shown in Figure 24. A constant shear rate of 0.01 s^{-1} was applied for 30 seconds for each test, followed by a resting period of 5 minutes. For the water cement ratio 0.7, the peak of the shear stress increased from 4 Pa to 16 Pa with time. With the imposed shear rate, a viscoelastic solid behavior was observed until a peak stress was reached. This should be the static yield stress of cement grout. The shear stress decreased after the peak and reached a steady state. The first measurement at 5 minutes is believed to be measured during the early hydration of the cement suspension. The thixotropic structural buildup of the suspension might occur during the measurement. This could be the reason for a constant shear stress that followed after the peak stress. The yield stress increased with time, which was expected. In contrast to Figure 23, the direct measurements showed an increase of yield stress, which is due to the resting of the grout. Since the material was not sheared unlike the stress ramp tests, structural buildup and flocculation were more prominent here.

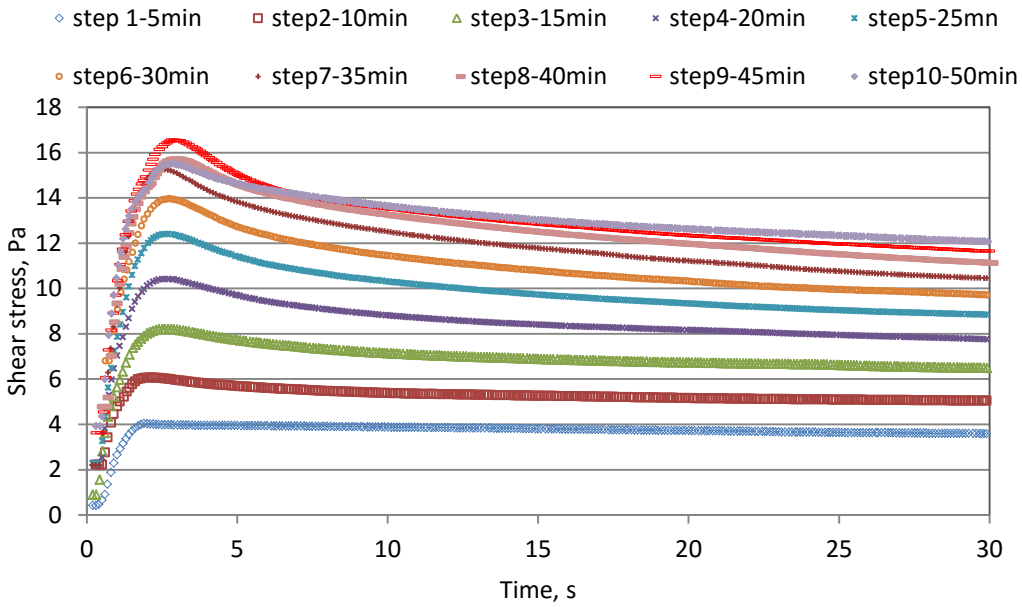

Figure 24 Shear stress at a constant shear rate of $0.01s^{-1}$ for w/c ratio 0.7

Thixotropic suspensions show a discontinuous change of the viscosity below and above the yield stress. Creep tests were therefore performed to determine the yield stress and investigate the behavior of cement grout at different imposed stresses. Due to the thixotropic behavior of the cement grout below a critical stress, i.e., yield stress, the suspension stops flowing and, above this flows rapidly. The creep tests were performed for an imposed stress of 0.2, 1, 3, 5, 6.5 and 8 Pa. The change in viscosity for different imposed stress can be seen in Figure 25. As shown in the figure, for an imposed stress of 0.2, 1, 3 and 5 Pa, the viscosity increased with time until the grout reached a zero flow condition. The viscosity at steady state would be infinite. In contrast, for an imposed stress of 6.5 Pa and 8 Pa, the viscosity decreased and was followed by a finite value at steady state. The change of viscosity corresponding to an applied stress of 5 and 6.5 Pa was discontinuous therefore, there remains a critical stress between 5 and 6.5 Pa that governs whether the material would lead to a zero flow due to aging with time or lead to a rapid flow due to the breakdown of the particle bonding, i.e., shear rejuvenation. For an applied stress of 6.5 Pa, the viscosity initially increased but decreased to a finite viscosity after a certain time. At the initial stage of the imposed stress, the viscosity increased due to aging however, inter particle bonds were destroyed after a certain time and the viscosity decreased. For thixotropic suspensions, e.g., cement grout, there is always a competition between the structural buildup, i.e., aging and break down, i.e. shear rejuvenation of the particles and the change are abrupt at yield stress, as shown in the Figure 25. As can be seen in this figure, cement grout showed a bifurcation behavior of viscosity at the yield stress. It can be concluded that the static yield stress was between 5- 6.5 Pa.

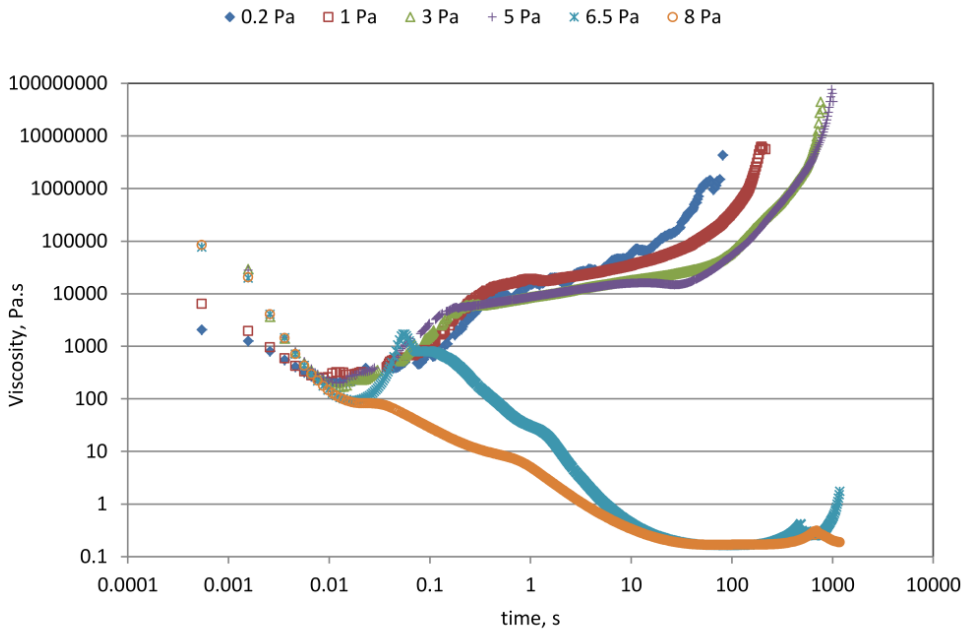

Figure 25 Static yield stress determined by creep tests

4.4.2 Measurement of dynamic yield stress

The dynamic yield stress was measured after applying a pre shear in order to achieve a broken down state of the cement particles. Stress ramp tests were performed and the down ramp, e.g., an applied stress of 15 -0 Pa, was applied. The determined yield stress was therefore the dynamic yield stress. The results are shown in Figure 26. In contrast to the up curve, a lower apparent viscosity and yield stress was observed, which was due to thixotropy. The dynamic yield stress for a water cement ratio of 0.7 increased with time, although over a very small magnitude. The sample was subjected to a stress ramp from 0 Pa-15 Pa each 5 minutes. This implies that the particle bonding was broken due to shearing, which might influence the aging of the material. As a consequence, the effect of aging for grout would not be the same as it would be if stress was not imposed at every 5 minutes. it could thus be said that the sample was at a semi disturbed state. It can be concluded from Figure 26 that the dynamic yield stress was in a range of 2.5 -3 Pa.

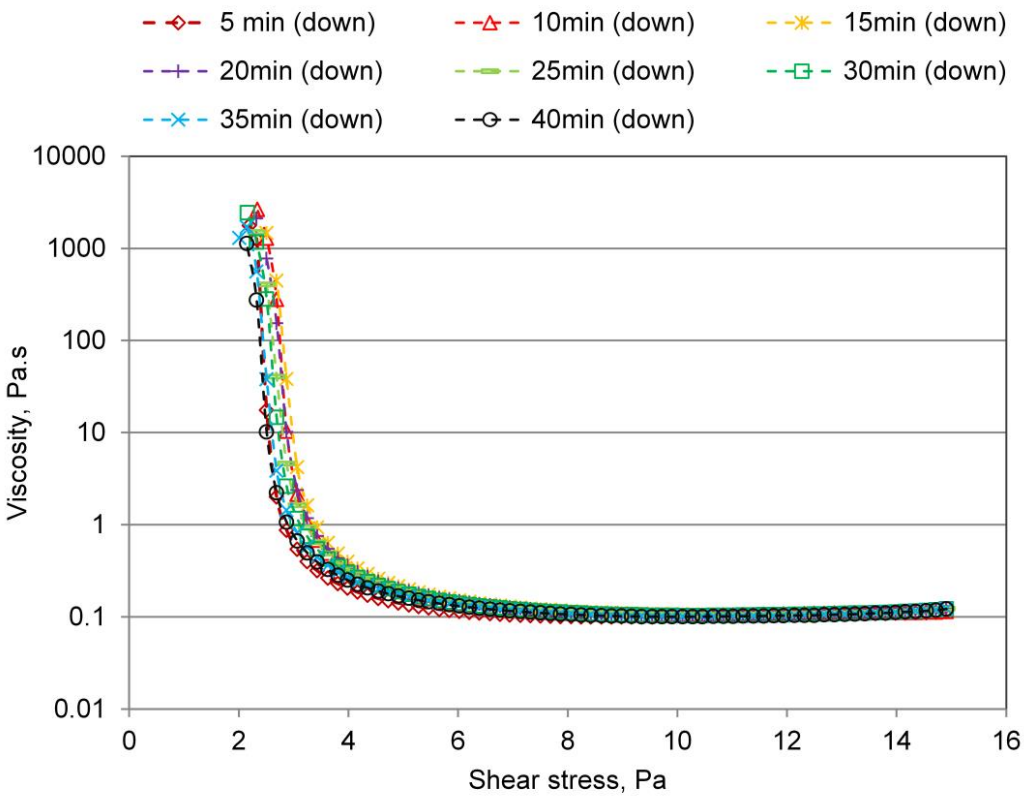

Figure 26 Dynamic yield stress determined by stress ramp tests

Stress relaxation tests were done in order to determine the dynamic yield stress of cement grout for a w/c ratio of 0.7. Tests were made for 3 different rotational speeds, 10 rpm, 100 rpm, and 200 rpm and the results are shown in Figure 27. The concentric cylinder was rotated at the specified rotational speed and stopped after a certain time. The residual stress left at the cylinder was regarded as the dynamic yield stress. As shown in the Figure 27, a lower dynamic yield stress was observed for a higher rotational speed, e.g. 100 rpm and 200 rpm in comparison to 10 rpm. This can be explained by particle migration during the rotation. A rotational speed of 10 rpm resulted in a higher dynamic yield stress and an increase with time. This implies that a breakdown of the particle bonds was not achieved at this particular rotation speed and that the yield stress increased with time due to hydration. In contrast, for the higher rotational speeds, the resting period was not sufficient to reform the particle bonding; therefore, a lower dynamic yield stress was achieved. it can be seen in Figure 27 that the rotational speed of 100 rpm provided reasonable results for dynamic yield stress of cement grout, in comparison to the results determined by the stress ramp tests as shown in Figure 26.

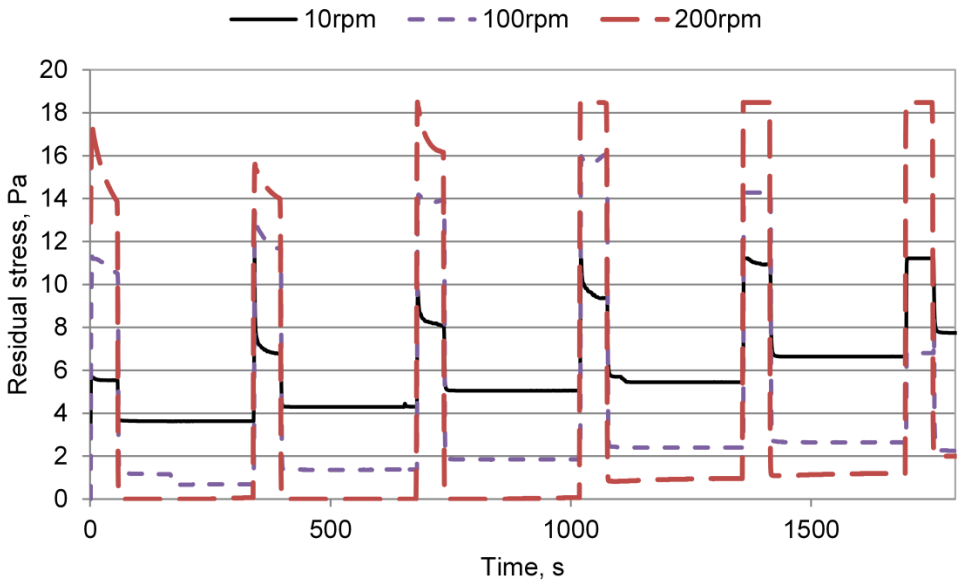

Figure 27 Dynamic yield stress measured by the stress relaxation test for w/c 0.7

In –line measurements were made using the Ultrasound Velocity profiling combined with the Pressure Difference (UVP+PD) method in order to determine the yield stress while the grout was pumped in an experimental flow loop. The determined yield stress should thus be regarded as the dynamic yield stress, i.e., at a broken down state which is similar to the grout at rock fractures. Velocity profiles were measured directly in-line for a water to cement ratio of 0.7 for different velocities, and no abrupt changes in the shape of the velocity profiles was observed. Therefore, the existence of a critical shear rate, i.e., shear banding, was not observed. The changes in the pressure difference, wall shear rate and plug radius for different pressure were measured. With an increased pressure, the pressure difference and the shear rate at the pipe wall were increased. As a consequence, the plug radius decreased. Figure 28 shows power law model parameters to explain the rheological behavior of cement grout inside the pipe. The yield stress was determined from the measured plug radius, and the rest of the flow curve was fitted using the power law model. However, it must be noted that the measured velocity profiles at low shear rates, e.g., near the plug, are most erroneous due to attenuation and it is therefore difficult to achieve a precise measurement. In addition, the measured plug radii at different pressure, e.g., velocity, were rather small, e.g., few mm and indicate the limitation of the measurement with respect to the accuracy of measuring a slight change of the plug radius. A slight discrepancy of the yield stress was thus observed. However, since cement grout is a complex suspension, this should be seen as a range for the dynamic yield stress instead of a single numerical value.

With increased velocity, the consistency index, k, decreased, which indicates that the viscosity decreased. Since cement grout shows a finite viscosity at higher stress, the consistency index, k should reach a certain value with an increased velocity. In addition, the flow index, n slightly increased, which indicates an increase of a shear thinning behavior. A non zero velocity at the pipe wall was measured, which indicates the existence of slip at the liquid-pipe wall interface.

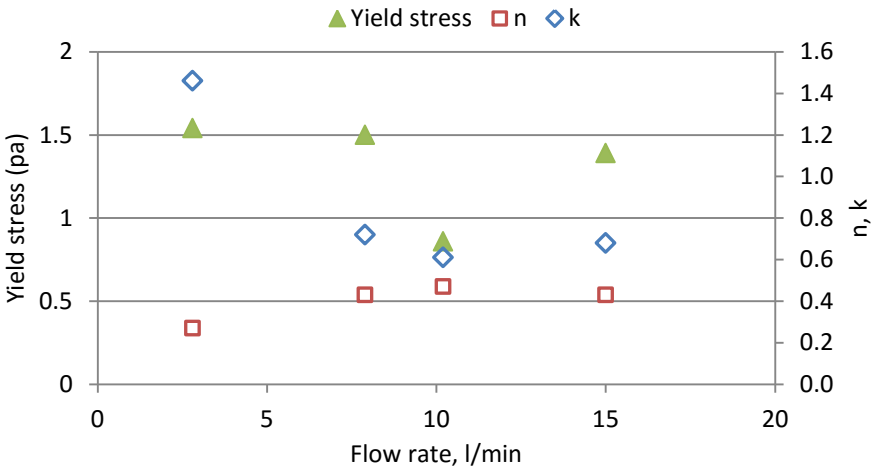

Figure 28 Yield stress and Power law model parameters for w/c ratio 0.7 determined by in-line measurements

4.4.3 Shear banding of cement grout

Shear banding is a phenomenon that occurs due to stress heterogeneity at low shear rates for thixotropic fluids (Ovarlez et al. 2009). The difference between simple yield stress fluid, i.e., H-B fluid and thixotropic fluid, i.e., cement grout, is that the shear rate changes to approximately zero abruptly at a sufficiently low shear rate for a thixotropic fluid. Below a critical stress, i.e., yield stress, the shear stress is heterogeneous.

Comparisons of flow curves at imposed stress and imposed rate, performed off-line are shown in Figure 29. For the up curve, the measurements were performed after the grout was at rest for 5 minutes and 10 minutes after mixing and was therefore subjected to build up. As shown in the figure, the controlled stress measurement provided a smooth curve, which represents the viscous behavior of a suspension. However, the controlled rate measurements showed a discontinuous change of the shear stress for a shear rate of 1.0 and below. An unsteady distribution of shear stress was observed up to the lowest shear rate, measured by the rheometer. Therefore, this is the region, subjected to shear banding and the critical shear rate for this particular grout is approximately $1s^{-1}$. However, the overlapping of the flow curve, measured by controlled stress up to a shear rate 0.05 s^{-1} was not understood.

For the down curve, the measurements were performed when the imposed stress and rate were reduced to zero from a certain value. The measurements were thus performed when the particle bonds were destroyed and the associated yield stress should be regarded as the dynamic yield stress. As shown in Figure 29, the controlled stress and controlled rate both provided a smooth curve, and no discontinuous change was noted at approximately 0.1 s^{-1}.

The shear stress vs shear rate curves for cement grout, measured in-line, are shown in Figure 30. The shear rate was determined from the velocity profile, and the shear stress was determined from the momentum balance. Therefore, it is the actual measured rheological behavior of cement grout that is presented. The shear rate range was different for each curve due to a different velocity of the grout inside the pipe. At lower velocity, e.g., 3 liter/min, a comparatively higher shear stress was observed, which might be due to an increase in viscosity at this velocity. In addition, since no discontinuous behavior was observed, it can be said that cement grout behaves as a simple yield stress fluid, i.e., an H-B fluid at a broken down state. This finding is in good agreement with the results shown for off-line measurements in figure 29. This can be further validated in Figure 31, where a spectral image of the velocity profile for a w/c ratio of 0.7 is shown. Due to a high spatial resolution of the Flow-Viz pulser receiver hardware, an accurate measurement of the velocity profile was made and visualized. As shown in the figure, no abrupt change was seen. Furthermore, the spectral image shows that a penetration depth larger than the center of the pipe was achieved and a plug flow can be visualized. The velocity profile near the far wall was distorted due to attenuation of the grout.

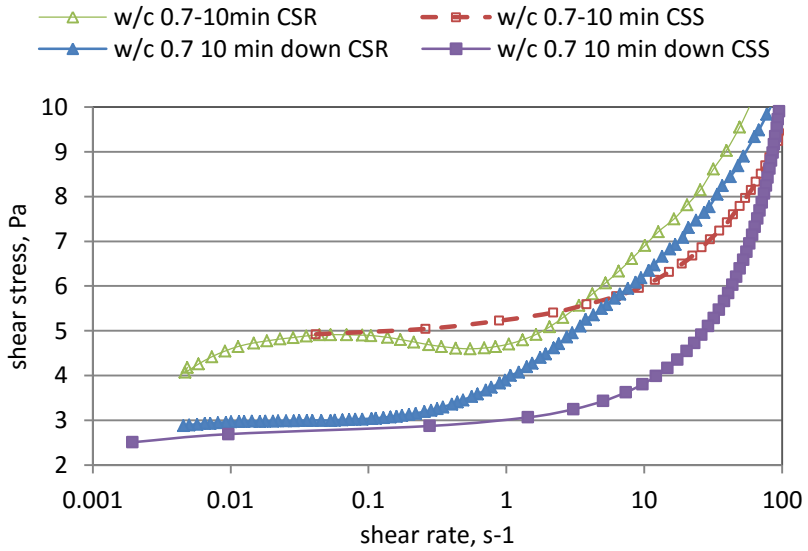

Figure 29 Flow curve for w/c ratio 0.7 after resting, i.e. aging at up curve and break down, i.e., shear rejuvenation at down curve

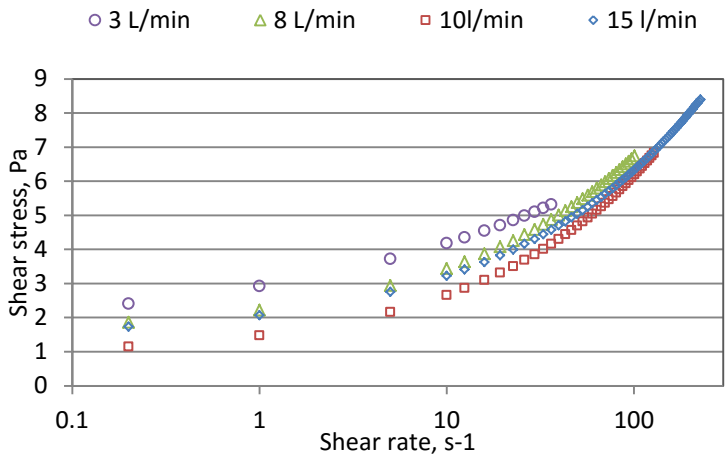

Figure 30 Shear stress vs shear rate measured in-line for w/c ratio 0.7

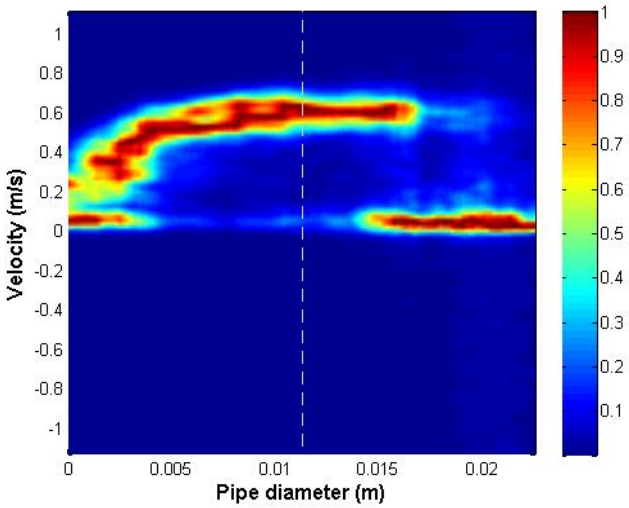

Figure 31 Spectral image of the velocity profile for w/c ratio 0.7

4.4.4 Comparison of static and dynamic yield stress

Comparison of static and dynamic yield stress for a water cement ratio of 0.7 of cement grout is shown in Figure 32. The static yield stress was determined by the stress ramp tests, vane method and creep tests, and the dynamic yield stress was determined by the stress ramp tests, stress relaxation tests and UVP+PD method.

For stress ramp tests, the yield stress determined from the up-ramp, i.e., when the applied stress was increased from 0 Pa -15 Pa, is the static yield stress. In contrast, the yield stress determined from the down ramp, i.e., when the sample was sheared, is the dynamic yield stress. The yield stress determined by the vane method was achieved at a very low shear rate;

it is therefore the static yield stress. In contrast, the stress relaxation test provided the residual stress after shearing the material; therefore, it is the dynamic yield stress. Shear rate ranges for the stress ramp tests are chosen from the corresponding flow curves shown in Figure 29.

Shear banding; i.e., non homogeneous distribution of the shear, was possibly observed at the up curve for a shear rate lower than 0.1 s^{-1}. A linear increase of shear stress was observed until 0.1s-1 followed by gradual breakage of the bonding. A nonlinear increase of shear stress i.e., an abrupt decrease of viscosity was observed for shear rates from 0.1 s-1 to 10 s-1; this is therefore considered to be the transition zone. However, a rapid increase of shear stress with an increased shear rate was observed for shear rates above 10s^{-1}. Subsequently, a finite viscosity was determined. Therefore, this was the dynamic yield stress of cement grout. Even though there are small discrepancies between the yield stress values determined by different methods, this should be ignored because of different measurement techniques. In addition, the difference is very small. However, it must be noted that the different phenomena, e.g., shear localization, shear banding and aging have consequences for the shear rate. The range of shear rate for static yield stress should thus be decided with care.

The static and dynamic yield stress with corresponding shear rate ranges is of great importance for grouting applications because it is used as an input for designing the grouting time and spread. It can be assumed from Figure 32 that cement grout is at a broken down state inside the rock fracture during pumping. Therefore, the dynamic yield stress should be used for designing the stop criteria. However, when the grout reaches the maximum penetration length, the static yield stress might be approached due to the decrease in velocity. In addition, static yield stress should be used as a design value when there is a sudden stop during the pumping of grout. In recent grouting stop criteria theories, the maximum penetration length is calculated on the basis of a constant value of the yield stress. However, It is evident in Figure 25 that the grout will stop sooner, resulting in a lower penetration due to the viscosity bifurcation of cement grout, i.e. a transition of yield stress from dynamic to static owing to the change of the velocity.

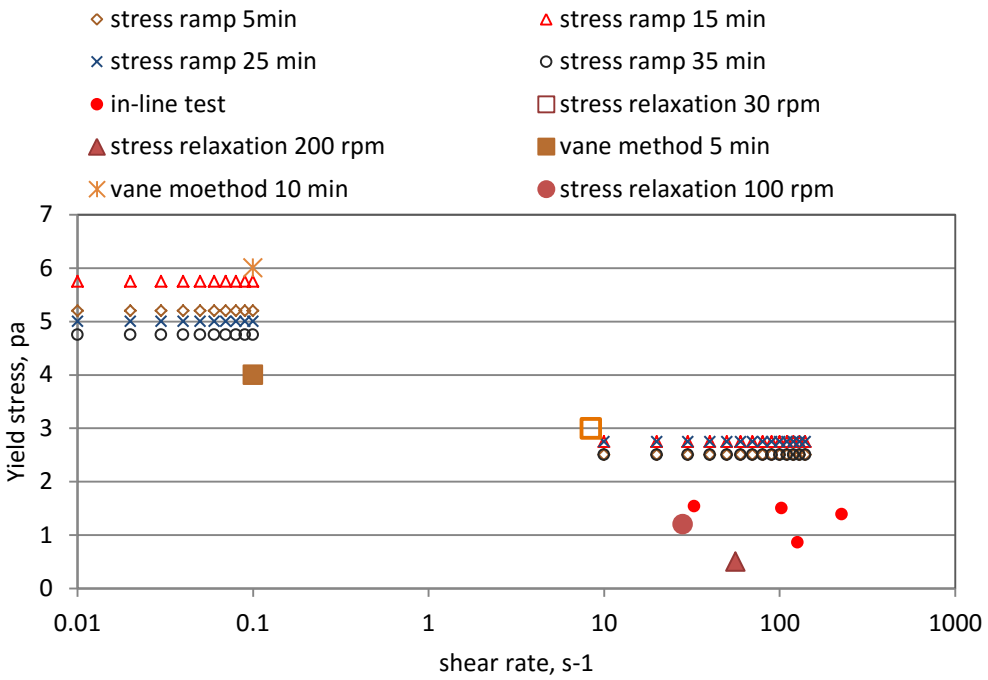

Figure 32 Comparison of static and dynamic yield stress of cement grout of w/c ratio 0.7

4.4.5 Wall slip phenomenon and yield stress

A wall slip phenomenon is inevitable for the flow of suspensions in a smooth geometry (Barnes 1995). The magnitude of the slip depends on the stress applied. Well above the yield stress, slip is negligible compared to the bulk flow. Just above the yield stress, slip becomes significant and the total deformation results from a combination of bulk flow and slip. Below the yield stress, the bulk flow is negligible and the apparent motion is entirely due to wall slip (Bertola et al. 2003; Meeker et al. 2004). However, these studies were performed using different geometries, e.g., concentric cylinder and parallel plate of conventional off-line rheometry. Slip was therefore observed at the smooth surface of the geometry, and a decreased apparent viscosity was measured. In contrast, in this work, the velocity profiles were visualized and the yield stress was determined from the measured plug radius. Normalized velocity profiles for a water cement ratio of 0.7 at different flow rates are shown in Figure 33. As shown in the figure, slip at the wall indeed exists, and the slip velocity decreased with an increased flow rate. Furthermore, the plug radius was decreased and the change of the shape of the velocity profile can be visualized. The measured plug radii for different water cement ratios at different flow rates are shown in Figure 34. The change of the plug radius was not consistent. This can be explained by the fact that the magnitude of the plug depends on the applied pressure and the slip at the wall and, therefore on the change of the shape of the velocity profile.

In addition, the yield stress of cement grout is not a single numerical value; rather a range of values due to the thixotropic behavior. Therefore, a slight inconsistency of the plug radius is reasonable. The corresponding yield stresses are shown in Figure 28.With an increased flow rate, the change of the pressure drop and wall shear rate was measured. This is shown in Figure 35. With an increased flow rate, the pressure drop and the wall shear rate increased. The increase of the wall shear rate indicates that the shape of the velocity profile is changing from a Bingham to a H-B model. This is in good agreement with Meeker et al. (2004). However, the shear stress generated at the lowest applied flow rate was well above the yield stress, therefore, the change in the shape of the velocity profile due to wall slip was not well understood.

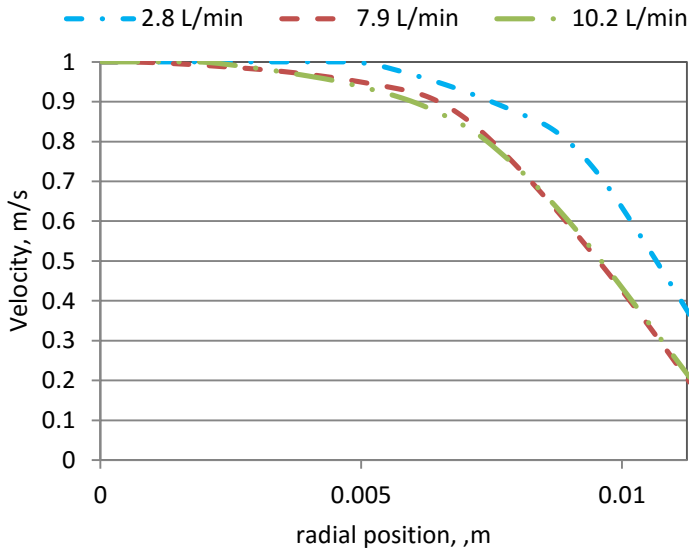

Figure 33 Measured velocity profiles for w/c ratio 0.7

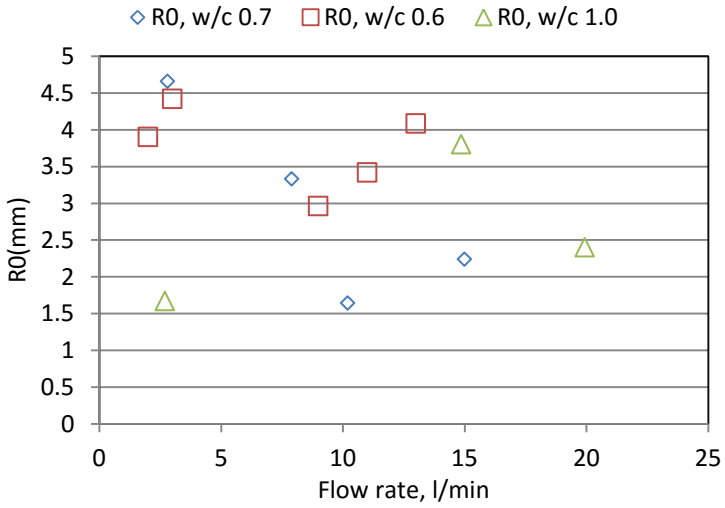

Figure 34 Measured plug radius for w/c ratio 0.6, 0.7 and 1.0

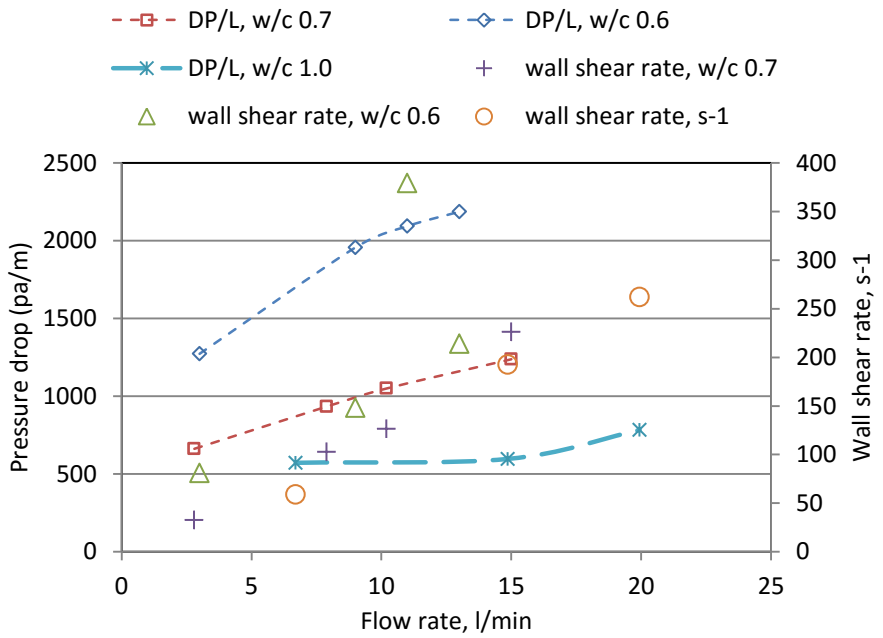

Figure 35 Change of pressure drop and wall shear rate for w/c ratio 0.6, 0.7 and 1.0

4.5 Estimation of shear rate, velocity and plug thickness of cement grout (Paper IV)

The yield stress is required as a design input to be able to estimate the spread of grout using the RTGC method. To decide the static or dynamic yield stress as a design input, the shear rate needs to be estimated. Estimation of the plug thickness is 'a priori' for determining the shear rate. An explicit analytical solution for estimating the plug thickness is available for one dimensional flow. However, the plug thickness for a two dimensional flow can only be estimated numerically. Therefore, in this work the approximate analytical solution for relative grout spread I_D as a function of relative time t_D from Gustafson and Stille (2005) was used to obtain the solution for plug thickness for radial flow.

To determine the Bingham number (B_N) and the velocity for two dimensional flow, the analytical expression for the derivative $\frac{dI_D}{dt_D}$ is required. Since I_D is the relative penetration of grout in a relative time t_D, $\frac{dI_D}{dt_D}$ can be defined as the dimensionless velocity. $\frac{dI_D}{dt_D}$ is a function of relative time, t_D and can be shown as

$$\frac{dI_D}{dt_D} = \frac{\delta}{2(t_D+\delta)^2}\left(\frac{\frac{t_D}{2\left[t_D+\delta\right]}+2}{\sqrt{\frac{2t_D}{\left[t_D+\delta\right]}+\left[\frac{t_D}{2\left(t_D+\delta\right)}\right]^2}} -1 \right) \tag{33}$$

4.5.1 Comparison of grout spread for different geometries

Calculations were performed for a one dimensional circular pipe, rectangular channel and a two dimensional radial disk. The material properties and other information are shown in Table 1 and Table 2, respectively. For a one dimensional geometry of a pipe and rectangular channel, explicit analytical solutions were used (Gustafson and Claesson, 2005) . Approximate analytical solutions by Gustafson and Stille (2005) and El Tani (2013) were used for a two dimensional radial disk. In addition, numerical calculations were performed for a radial disk following Hässler (1991).

Table 2 Water/cement ratio and rheological properties

w/c ratio	Yield stress (pa)	Viscosity (mPas)
0.8	5	25

Table 3 Design parameters

Fracture aperture (μm)	Grout pressure (MPa)	Required spread of grout (m)
100	1	2.5

For flow in a circular pipe, the diameter used was the same as the fracture aperture, *b*. The characteristic grouting time will be $t_0 = 24000$ s, and the maximum spread of grout will be $I_{max} = 10$ m. Therefore, the relative penetration for the required grout spread is $I_D = 0.25$. The relative spread of grout with respect to the relative time is shown in Figure 36. For a radial spread, a longer time is required in order to achieve the same length of grout spread in comparison to a one dimensional pipe and channel. In practice, the spread of grout is probably somewhere between the one dimensional and two dimensional geometry. From Figure 36, the required grouting time can be determined according to the required spread of grout, with respect to the maximum spread, and was estimated as *t*=6 min for circular pipe, *t*=10 min for a rectangular channel and *t*= 40 min for a radial disk. Numerical calculations were in good agreement with the approximate solutions, which validate the applicability of the approximate solution for further derivation of the dimensionless velocity, plug thickness and shear rate.

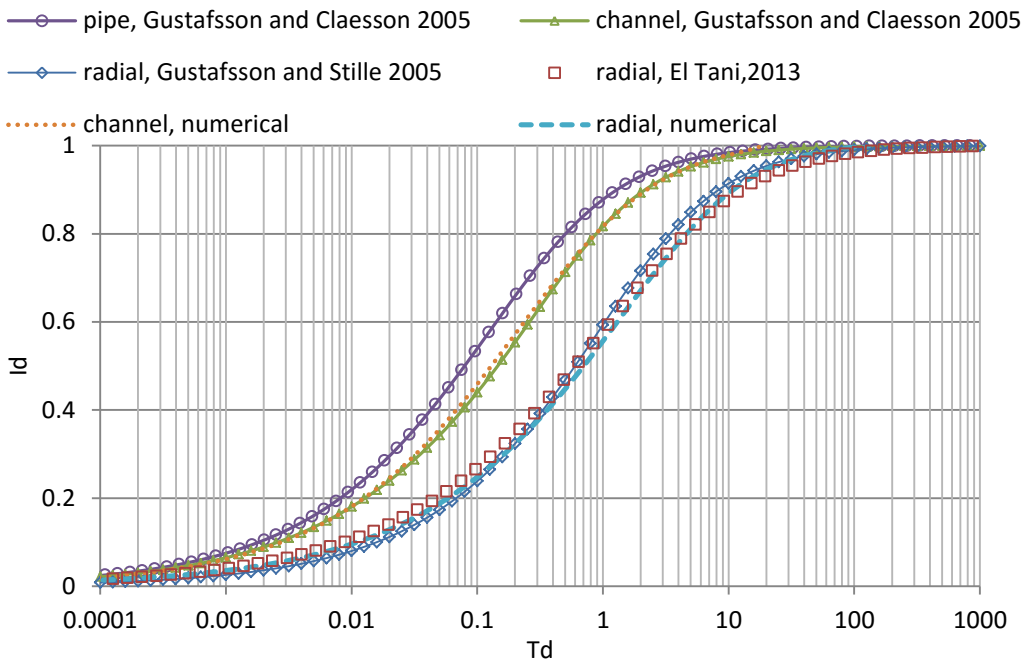

Figure 36 Relative spread of grout in relative time for a circular pipe, rectangular channel and radial disk

The B_N was estimated and is shown in Figure 37. For a one dimensional pipe and channel, explicit analytical solutions shown in equations 21 and 22 were used. However, for radial flow, the Bingham Number was obtained as a function of $\frac{dI_D}{dt_D}$ and the corresponding I_D values were used to plot Figure 37. The results obtained by numerical calculations are in good agreement with the analytical approach. Therefore, the approximate analytical solution for calculation of B_N is further validated. The significance of this B_N is that, by using the B_N from Figure 37, the plug thickness can be determined for the corresponding relative spread of grout.

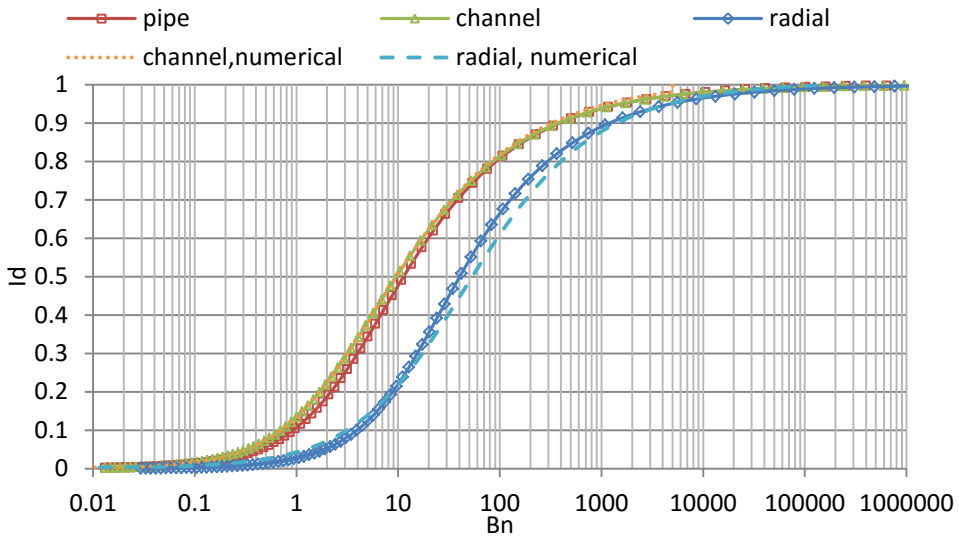

Figure 37 Bingham Number of cement grout in a rectangular channel and radial disk

The plug thickness of the grout front for different geometries was determined and is shown in Figure 38. For a one dimensional geometry, the increase of the plug is linear with respect to the spread of grout. However, for a two dimensional geometry, the change of the plug is non linear and could not be solved analytically in earlier works (Hässler 1991). The non linearity of the change of the plug thickness is due to the change in the pressure difference, which is a function of the radial distance. In this work, this is the first time the change of the relative plug thickness was determined 'semi analytically'.

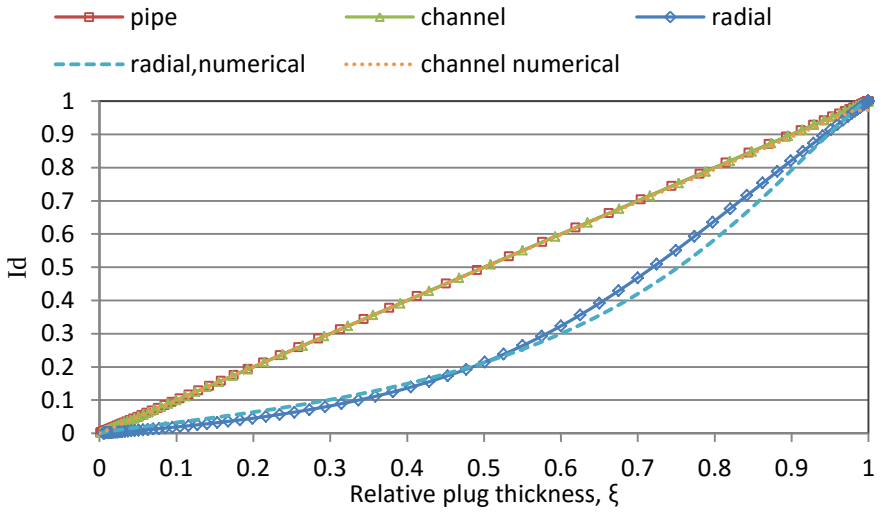

Figure 38 Relative plug thickness of grout for a circular pipe, rectangular channel and radial disk

The dimensionless shear rate was estimated from the relative plug thickness using equation 32 and is shown in Figure 39. The estimated dimensionless shear rate, shown in Figure 39, is

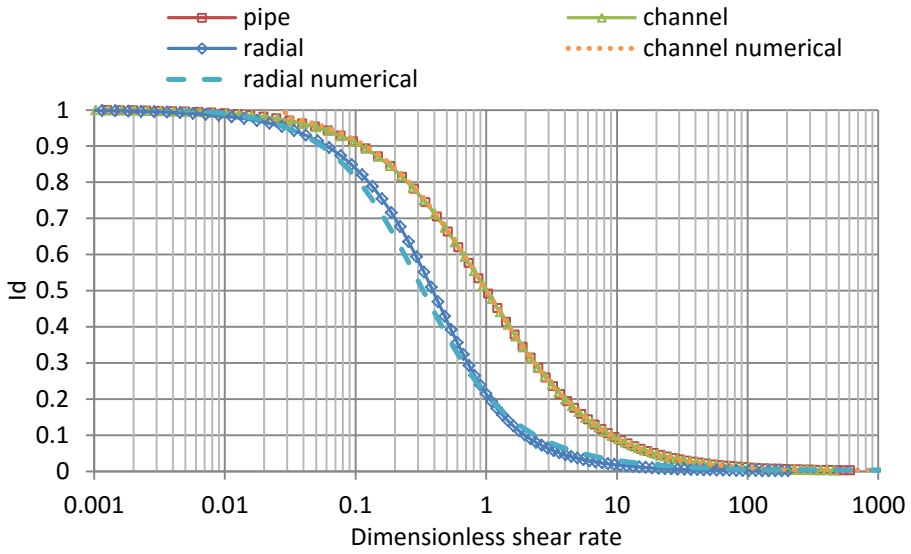

Figure 39 Dimensionless shear rate of grout for different geometries

independent of the rheological properties and depends only on the relative plug thickness; therefore, it can be regarded as a unique graph. To obtain the real shear rate, it must to be multiplied by $\frac{\tau_0}{\mu_B}$.

4.5.2 Development of a non dimensional nomogram for the estimation of plug thickness, velocity and shear rate

In this work, a non dimensional nomogram, based on the relative spread of grout was developed to estimate the plug thickness, velocity and shear rate in a one dimensional and two dimensional geometry. The procedure for determining the shear rate in a graphical method is shown in Figure 40, based on which the appropriate yield stress can be chosen. The design value of yield stress, i.e., static or dynamic yield stress should be decided on the basis of the shear rate subjected on the grout at the desired penetration length. The relative penetration length, I_D, should be determined for the corresponding geometry, which will led to the required time, t, to achieve the maximum spread of grout. However, the grouting pressure and material properties must to be optimized with respect to the estimated velocity, i.e., shear rate for the required spread of grout. The grouting time should be designed such a way that the shear rate of grout at the maximum required spread is sufficient to overcome the effect of aging. Therefore, a shear rate higher than 10 s^{-1} for a water cement ratio of 0.7 should be maintained at the desired spread of grout. This is due to the fact that a shear rate approximately less than 10 s^{-1} would lead to the aging of grout and eventually increase the yield stress, i.e., static yield stress. In addition, due to the shear thinning behavior of grout, the viscosity will increase. However, the shear rate margin for the transition of static

to dynamic yield stress would differ depending on the types of cement and concentration. As shown in Figure 40, when the relative spread of grout is known, the corresponding Bingham number and dimensionless shear rate can be determined from the corresponding graphs. In addition, the velocity can be determined from the Bingham number. The advantage of using the nomogram is that the curves are unique and the parameters are independent of the material properties, pressure and aperture.

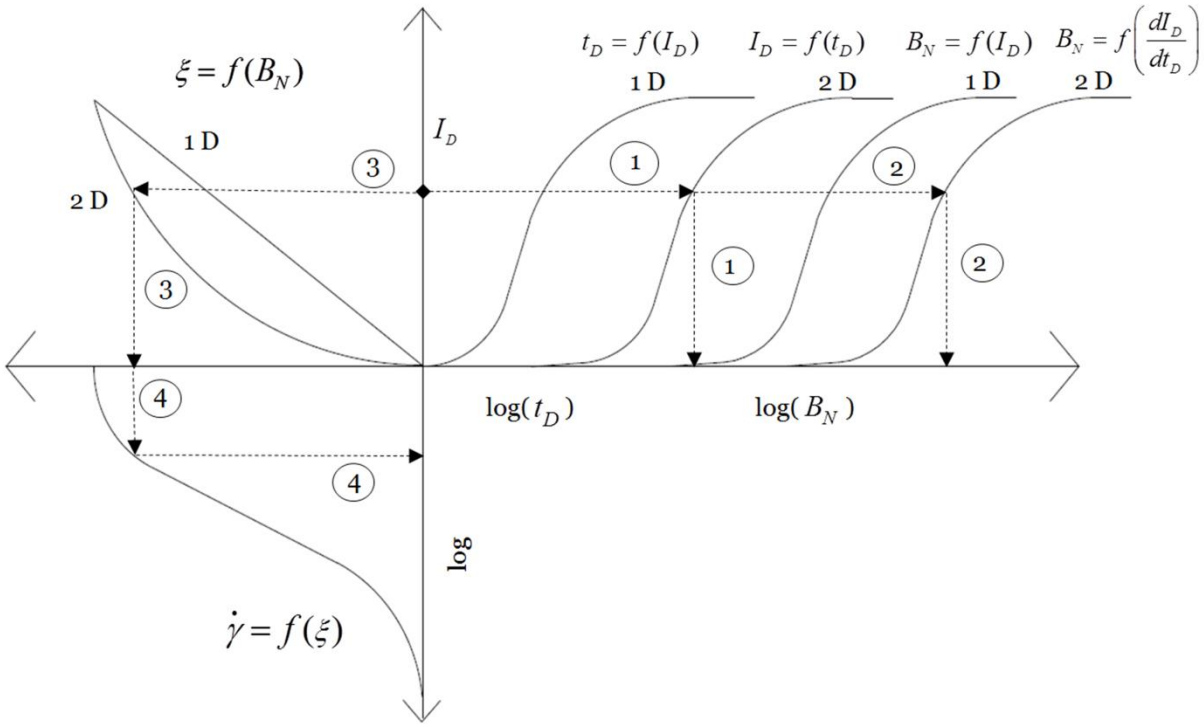

Figure 40 Graphical method to estimate the plug thickness, shear rate and velocity of grout

5 Conclusions and future outlook

5.1 Conclusions

The results obtained using the UVP+PD method were found to be very promising for direct in-line determination of the rheological properties of cement based grouts. It was subsequently found feasible to perform non invasive measurements through a high grade stainless steel pipe. It was possible to obtain the velocity profiles for a w/c ratio down to 0.6 and to determine the rheological properties, such as viscosity and yield stress. In addition to curve fitting with mathematical models such as Bingham and Herschel-Bulkley, a non-model approach was also applied. It was found that, with the non-model approach, the true velocity profile can be obtained. The volumetric flow rate was readily available by integration of the velocity profiles.

Measurements of yield stress showed that two ranges of yield stress, static and dynamic, indeed exist for the cement grout. The static and dynamic yield stress for different water to cement ratios were measured using different measurement techniques, and the critical shear rate to distinguish between static and dynamic yield stress was defined. During practical grouting applications, the shear rate changes from very high to low shear rates; therefore, it can be concluded that corresponding static and dynamic yield stresses should be used as a design parameter to determine the stop criteria of grouting work. In addition, the spread of grout would stop sooner than the estimated time due to the viscosity bifurcation, when the shear stress generated is equivalent to or lower than the critical stress.

To facilitate the estimation of the plug thickness, shear rate and velocity at the grout front in a two dimensional flow, a non dimensional parameter, the Bingham number (Bn), was used, which is the governing factor for the determination of the plug thickness and velocity of Bingham fluid flow. It was shown that the plug thickness, velocity and shear rate can be estimated semi analytically, and good agreement was found with numerical calculations.

The conclusions that can be drawn from this study are as follows:

1. It is possible to determine the rheological properties of cement grouts directly in-line under field conditions.

2. It is possible to determine the change of the rheological properties of cement grouts with concentration and time.

3. The yield stress and viscosity of cement grouts can be determined regardless of the rheological model.

4. The Flow-Viz pulser receiver unit combining the non-invasive sensor unit is capable of generating acoustic energy sufficient to measure velocity profiles beyond the center of the pipe; providing a spatial resolution of 11 micro meters. Therefore, detailed information on the velocity profile can be obtained.

5. The volumetric flow rate can also be accurately determined when the flow is very low.

6. The grout pump characteristics can be readily visualized.

7. The static yield stress of cement grout for a water to cement ratio of 0.7 was found to be in a range of 4 Pa – 6 Pa and the dynamic yield stress was found to be in a range of 1 Pa -3 Pa, for a time period of 35 minutes. The shear rate range for static yield stress was found to be 0.001 s^{-1} - 1 s^{-1} and the shear rate range for dynamic yield stress was found above 10 s^{-1} for cement grout with a water to cement ratio of 0.7.

8. Creep tests performed using the vane method showed that there exists a critical shear stress above which the grout flows with a viscosity that decreases to a constant value at steady state. However, at lower shear stresses, it was observed that the grout moves towards a no flow condition. Therefore, the suspension showed a bifurcation behavior and the critical shear stress, i.e., yield stress, for a water to cement ratio of 0.7 was found to be between 5 Pa and 6.5 Pa.

9. An unsteady flowing condition was observed for a shear rate less than $1s^{-1}$, which indicates the possible presence of shear banding at lower shear rates. In contrast to the off-line measurements, no discontinuous behavior was observed at low shear rates during in-line measurements. This implies that the grout behaves in a way similar to a simple yield stress fluid at broken down state and shows shear banding when it is subjected to aging.

10. The change in yield stress with time due to hydration was determined and it was found that the yield stress increases until the first 5 minutes and a decrease follows

afterwards, as seen in the change of the rate of heat evolution of the grout mix. However a gradual increase in the yield stress was observed after 10 minutes.

11. A nomogram consisting non dimensional parameters was developed that illustrates the key features and governing factors for grouting design. Using the nomogram the plug thickness, shear rate and velocity can be estimated for a cement grout. Based on the shear rate at the grout front, the design value of yield stress can be decided.

5.2 Recommendations for future works

The UVP+PD method is a novel application for the construction industry, and further research should be carried out to implement the technology in this field. A field test is required to validate the Flow-Viz system for field grouting rigs. Successful implementation of the Flow-Viz industrial rheometer in grouting rigs will lead to real time monitoring of the rheological properties of grout. Subsequently, the rheological properties can be updated to the RTGC algorithm and the spread of grout can be estimated in real time. The ultimate goal is that this method should be available in the field for continuous determination of the rheological properties and for quality control.

The UVP+PD method can be used to investigate the critical shear rate of cement grout at low shear rates due to the high spatial resolution. Further research should be performed to characterize the critical shear rate of cement grout for different concentrations and its effect on the grout spread.

A wall slip phenomenon is significant for the determination of the viscosity of cement grout. Ultrasound Velocity Profiling is an effective tool for investigating the velocity profiles at the near wall region. The shape of the velocity profile is changed due to a slip at the wall and the plug radius would consequently be changed. However, further research is required to visualize the change of the shape of the velocity profiles at different velocities.

Further work is required to investigate the spread of grout, and the velocity and shear rate for geometries between one dimension and two dimensions, which is often the case during grouting of rock fractures. In addition, in-line measurements with ultrasound should be made to validate the plug thickness of cement grout in two dimensional radial flow.

The change of the plug thickness for a radial flow can be visualized using the ultrasound velocity profiling and should be further investigated. The measurement of the plug thickness would be useful to verify the nature of plug flow, i.e., if it is constant or increased with an increased spread of grout inside radial disk geometry.

6 References

Abdali SS, Mitsoulis E, Markatos NC (1992) Entry and exit flows of Bingham fluids. Journal of Rheology (1978-present) 36:389–407.

Akroyd T, Nguyen Q (2003) Continuous rheometry for industrial slurries. Experimental Thermal and Fluid Science 27:507–514.

Axelsson M, Gustafson G (2006) A robust method to determine the shear strength of cement-based injection grouts in the field. Tunnelling and Underground Space Technology 21:499–503.

Banfill P (2006) Rheology of fresh cement and concrete. Rheology Reviews 31–130.

Banfill P (2003) The rheology of fresh cement and concrete - a review. In: Proceeding of 11th International Cement Chemistry Congress, Durban.

Barnes HA, Walters K (1985) The yield stress myth? Rheologica Acta 24: 323-326.

Barnes HA (1999) The yield stress–a review or [□][pi][alpha][nu][tau][alpha][rho][iota]'–everything flows? Journal of Non-Newtonian Fluid Mechanics 81:133–178.

Barnes HA (1997) Thixotropy–a review. Journal of Non-Newtonian Fluid Mechanics 70:1–33.

Barnes HA (1995) A review of the slip (wall depletion) of polymer solutions, emulsions and particle suspensions in viscometers: its cause, character and cure. J Non-Newtonian Fluid Mech 56:221–231.

Barnes HA, Hutton J, Walters K (1989) An introduction to rheology. Elsevier

Barnes HA, Nguyen QD (2001) Rotating vane rheometry–a review. Journal of Non-Newtonian Fluid Mechanics 98:1–14.

Bertola V, Bertrand F, Tabuteau H, et al (2003) Wall slip and yielding in pasty materials. Journal of Rheology (1978-present) 47:1211–1226.

Bird B, Dai GC, Yarusso BJ (1983) Rheology and flow of viscoplastic materials. Reviews in Chemical Engineering 1:1–70.

Bird B, Stewart E, Lightfoot N (1960) Transport Phenomena. Wiley and sons, New York.

Birkhofer B (2007) Ultrasonic In-line characterization of Suspensions. Doctoral Thesis, ETH.

Bonn D, Tanaka H, Coussot P, Meunier J (2004) Ageing, shear rejuvenation and avalanches in soft glassy materials. J Phys: Condens Matter 16:S4987.

Bukhman YA, Lipatov VI, Litvinov AI, et al (1982) Rehodynamics of nonlinear viscoplastic media. Journal of Non-Newtonian Fluid Mechanics 10:215–233.

Coussot P, Nguyen QD, Huynh HT, Bonn D (2002a) Avalanche behavior in yield stress fluids. Physical review letters 88:175501.

Coussot P, Nguyen QD, Huynh HT, Bonn D (2002b) Viscosity bifurcation in thixotropic, yielding fluids. Journal of Rheology (1978-present) 46:573–589.

De Larrard F, Ferraris CF, Sedran T (1998) Fresh concrete: a Herschel-Bulkley material. Materials and Structures 31:494–498.

El Tani M (2012) Grouting Rock Fractures with Cement Grout. Rock Mechanics and Rock Engineering 45:547–561.

El Tani M (2013) Grouting emancipation. The Grout Line 32–38.

Ferraris CF, Brower LE, Banfill PFG, et al (2001) Comparison of concrete rheometers: International tests at LCPC (Nantes, France) in October, 2000. US Department of Commerce, National Institute of Standards and Technology

Ferraris CF, Martys NS, George WL (2014) Development of standard reference materials for rheological measurements of cement-based materials. Cement and Concrete Composites 54:29–33

Gustafson G, Claesson J (2005) Steering parameters for rock grouting. Unpublished paper, submitted to International Journal of Rock Mechanics and Mining Sciemce.

Gustafson G, Claesson J, Fransson Å (2013) Steering Parameters for Rock Grouting. Journal of Applied Mathematics.

Gustafson G, Stille H (2005) Stop criteria for cement grouting. Felsbau 25:62–68.

Håkansson U (1993) Rheology of fresh cement based grouts. PhD Thesis, Royal Institute of Technology

Håkansson U, Rahman M (2009) Rheological properties of cement based grouts using the UVP-PD method. Nordic Symposium of Rock Grouting. Finnish Tunnelling Association, Helsinki.

Håkansson U, Hässler L, Stille H (1992) Rheological properties of microfine cement grouts. Tunnelling and Underground Space Technology 7:453–458.

Håkansson U, Rahman M, Wiklund J (2012) In-line measurements of rheological properties of cement based grouts- Introducing the UVP-PD method. In: Proceeding of 4th International Conference on Grouting and Deep Mixing, New Orleans

Hartnett JP, Hu RYZ (1989) Technical note: The yield stress—An engineering reality. Journal of Rheology (1978-present) 33:671–679.

Hässler L (1991) Grouting of rock - Simulation and Classification. PhD Thesis, KTH Royal Institute of Technology.

Hässler L, Håkansson U, Stille H (1992) Computer-simulated flow of grouts in jointed rock. Tunnelling and Underground Space Technology 7:441–446.

James AE, Williams DJA, Williams PR (1987) Direct measurement of static yield properties of cohesive suspensions. Rheologica acta 26:437–446.

Kobayashi S, Stille H, Gustafson G, Stille B (2008) Real time grouting control method - Development and application using ÄspÖ HRL data. R-08-133, Swedish Nuclear Fuel and Waste Management Co, Stockholm

Kotzé, R., Haldenwang, R., Slatter, P., 2008. Rheological characterization of highly concentrated mineral suspensions using ultrasonic velocity profiling combined pressure difference method. Applied Rheology 18, 62114.

Kotzé R, Wiklund J, Haldenwang R (2013) Optimisation of pulsed ultrasonic velocimetry system and transducer technology for industrial applications. Ultrasonics 53:459–469.

Liddel PV, Boger DV (1996) Yield stress measurements with the vane. Journal of non-newtonian fluid mechanics 63:235–261.

Lipscomb G, Denn M (1984) Flow of Bingham fluids in complex geometries. Journal of Non-Newtonian Fluid Mechanics 14:337–346.

Lombardi G (1985) Some theoretical considerations on cement rock grouting. Lombardi Engineering Ltd, In: Proceeding of Commission Internationale, Lussane.

Lombardi G, Deere D (1993) Grouting design and control using the GIN principle. International Water Power and Dam Construction.

Mannheimer RJ (1991) Laminar and turbulent flow of cement slurries in large diameter pipe: A comparison with laboratory viscometers. Journal of Rheology 35:113–133.

Meeker SP, Bonnecaze RT, Cloitre M (2004) Slip and flow in pastes of soft particles: Direct observation and rheology. Journal of Rheology 48:1295.

Moller P, Fall A, Chikkadi V, et al (2009a) An attempt to categorize yield stress fluid behaviour. Phil Trans R Soc A 367:5139–5155.

Moller P, Fall A, Bonn D (2009b) Origin of apparent viscosity in yield stress fluids below yielding. EPL 87:38004.

Mujumdar A, Beris AN, Metzner AB (2002) Transient phenomena in thixotropic systems. Journal of Non-Newtonian Fluid Mechanics 102:157–178.

Nehdi M, Rahman MA (2004) Estimating rheological properties of cement pastes using various rheological models for different test geometry, gap and surface friction. Cement and Concrete Research 34:1993–2007.

Nguyen QD, Akroyd T, De Kee DC, Zhu L (2006) Yield stress measurements in suspensions: an inter-laboratory study. Korea-Australia Rheology Journal 18:15–24.

Nguyen QD, Boger DV (1983) Yield stress measurement for concentrated suspensions. Journal of Rheology 27:321.

Nguyen QD, Boger DV (1985) Thixotropic behaviour of concentrated bauxite residue suspensions. Rheologica Acta 24:427–437.

Nguyen QD, Boger DV (1987) Characterization of yield stress fluids with concentric cylinder viscometers. Rheologica acta 26:508–515.

Ovarlez G, Rodts S, Chateau X, Coussot P (2009) Phenomenology and physical origin of shear localization and shear banding in complex fluids. Rheologica acta 48:831–844.

Papanastasiou TC (1987) Flows of Materials with Yield. Journal of Rheology 31:385.

Rahman M, Håkansson U, Wiklund J (2015) In-line rheological measurements of cement grouts: Effects of water/cement ratio and hydration. Tunnelling and Underground Space Technology 45:34–42.

Rahman M, Håkansson U, Wiklund J (2012) Grout pump characteristics evaluated with the Ultrasound Velocity profiling. In: Proceeding of International Symposium of Rock Mechanics, EUROCK, Stockholm.

Ricci S, Boni E, Guidi F, et al (2006) A programmable real-time system for development and test of new ultrasound investigation methods. Ultrasonics, Ferroelectrics, and Frequency Control, IEEE Transactions on 53:1813–1819.

Ricci S, Liard M, Birkhofer B, et al (2012) Embedded Doppler system for industrial in-line rheometry. IEEE Transactions on Ultrasonics, Ferroelectrics, and Frequency Control 59:1395–1401.

Rosquoët F, Alexis A, Khelidj A, Phelipot A (2003) Experimental study of cement grout. Cement and Concrete Research 33:713–722.

Sant G, Ferraris CF, Weiss J (2008) Rheological properties of cement pastes: A discussion of structure formation and mechanical property development. Cement and Concrete Research 38:1286–1296.

Schurz J (1990) The yield stress—an empirical reality. Rheologica acta 29:170–171.

Struble LJ, Schultz MA (1993) Using creep and recovery to study flow behavior of fresh cement paste. Cement and concrete research 23:1369–1379.

Takeda Y (1986) Velocity profile measurement by ultrasound Doppler shift method. International journal of heat and fluid flow 7:313–318.

Wallevik JE (2009) Rheological properties of cement paste: Thixotropic behavior and structural breakdown. Cement and Concrete Research 39:14–29.

Wallevik OH, Feys D, Wallevik JE, Khayat KH (2015) Avoiding inaccurate interpretations of rheological measurements for cement-based materials. Cement and Concrete Research, Article in Press.

Wiklund JA, Stading M, Pettersson AJ, Rasmuson A (2006) A comparative study of UVP and LDA techniques for pulp suspensions in pipe flow. AIChE Journal 52:484–495.

Wiklund J, Kotzé R, Haldenwang R, Stading M (2012) Development of an industrial UVP+ PD based rheometer-optimisation of UVP system and transducer technology. In: Proceeding of 8th International Symposium on Ultrasonic Doppler Methods for Fluid Mechanics and Fluid Engineering. Dresden.

Wiklund J, Shahram I, Stading M (2007) Methodology for in-line rheology by ultrasound Doppler velocity profiling and pressure difference techniques. Chemical Engineering Science 62:4277–4293.

Wallner M (1976) Propagation of sedimentation stable cement pastes in jointed rock. Rock mechanics and waterways construction 2:132–136.

Yahia A, Khayat KH (2003) Applicability of rheological models to high-performance grouts containing supplementary cementitious materials and viscosity enhancing admixture. Materials and Structures 36:402–412.